



Chinese Pharmaceutical Association
Institute of Materia Medica, Chinese Academy of Medical Sciences

Acta Pharmaceutica Sinica B

www.elsevier.com/locate/apsb
www.sciencedirect.com



REVIEW

Engineering nanomedicines for immunogenic eradication of cancer cells: Recent trends and synergistic approaches



Ahmed O. Elzoghby^{a,*}, Omar Samir^a, Hagar E. Emam^a,
Ahmed Soliman^a, Riham M. Abdelgalil^b, Yomna M. Elmorshedy^b,
Kadria A. Elkhodairy^b, Mahmoud L. Nasr^{a,*}

^aDivision of Engineering in Medicine and Division of Renal Medicine, Department of Medicine, Brigham and Women's Hospital, Harvard Medical School, Boston 02115, MA, USA

^bCancer Nanotechnology Research Laboratory (CNRL), Faculty of Pharmacy, Alexandria University, Alexandria 21521, Egypt

Received 1 August 2023; received in revised form 7 February 2024; accepted 9 March 2024

KEY WORDS

Immunogenic cell death;
Immunogenic eradication;
Nanomedicines;
Drug delivery;
Cancer immunotherapy;
Antitumor immunity;
T cells;
Tumor associated antigens;
Synergistic immune response

Abstract Resistance to cancer immunotherapy is mainly attributed to poor tumor immunogenicity as well as the immunosuppressive tumor microenvironment (TME) leading to failure of immune response. Numerous therapeutic strategies including chemotherapy, radiotherapy, photodynamic, photothermal, magnetic, chemodynamic, sonodynamic and oncolytic therapy, have been developed to induce immunogenic cell death (ICD) of cancer cells and thereby elicit immunogenicity and boost the antitumor immune response. However, many challenges hamper the clinical application of ICD inducers resulting in modest immunogenic response. Here, we outline the current state of using nanomedicines for boosting ICD of cancer cells. Moreover, synergistic approaches used in combination with ICD inducing nanomedicines for remodeling the TME *via* targeting immune checkpoints, phagocytosis, macrophage polarization, tumor hypoxia, autophagy and stromal modulation to enhance immunogenicity of dying cancer cells were analyzed. We further highlight the emerging trends of using nanomaterials for triggering amplified ICD-mediated antitumor immune responses. Endoplasmic reticulum localized ICD, focused ultrasound hyperthermia, cell membrane camouflaged nanomedicines, amplified reactive oxygen species (ROS) generation, metallo-immunotherapy, ion modulators and engineered bacteria are among the most innovative approaches. Various challenges, merits and demerits of ICD inducer nanomedicines were also discussed with shedding light on the future role of this technology in improving the outcomes of cancer immunotherapy.

*Corresponding authors.

E-mail addresses: aelzoghby@bwh.harvard.edu (Ahmed O. Elzoghby), mnasr@bwh.harvard.edu (Mahmoud L. Nasr).

Peer review under the responsibility of Chinese Pharmaceutical Association and Institute of Materia Medica, Chinese Academy of Medical Sciences.

<https://doi.org/10.1016/j.apsb.2024.03.022>

2211-3835 © 2024 The Authors. Published by Elsevier B.V. on behalf of Chinese Pharmaceutical Association and Institute of Materia Medica, Chinese Academy of Medical Sciences. This is an open access article under the CC BY-NC-ND license (<http://creativecommons.org/licenses/by-nc-nd/4.0/>).

1. Introduction

1.1. Challenges of cancer immunotherapy

Despite the approval of several immunotherapy drugs for cancer treatment, many patients are still not responding well to immunotherapy. A number of factors can explain the observed resistance to cancer immunotherapy including low ability of cancer cells to induce an immunogenic response, poor capacity of dendritic cells (DCs) to present tumor-associated antigens (TAAs), and low number of cytotoxic CD8⁺ T lymphocytes (CTLs) infiltrating the tumor^{1,2}. An immune-suppressive microenvironment is created by tumor and stromal cells through the production of suppressive cytokines and enzymes (*e.g.*, transforming growth factor β (TGF β), interleukin 10 (IL-10), and indoleamine 2,3-dioxygenase (IDO), and expression of inhibitory mediators [*e.g.*, programmed cell death ligand 1 (PD-L1) and Fas ligand (Fas L)]. Moreover, cancer cells also recruit and activate immunosuppressive cells, including regulatory T cells (Tregs), tumor-associated macrophages (TAMs), tolerogenic dendritic cells (DCs), and myeloid-derived suppressor cells (MDSCs)^{3,4}. As a result, cancer cell-specific T cells are inhibited within the tumor microenvironment (TME). Therefore, innovative strategies are needed to overcome those challenges and hence increase the responsiveness to cancer immunotherapy modalities.

1.2. Molecular mechanism of ICD

Immunogenic cell death (ICD) is an inflammatory response associated with special type of cell death that results in an enhanced anti-tumor immunity⁵. During ICD, cancer cells release TAAs together with damage-associated molecular patterns (DAMPs), such as adenosine triphosphate (ATP), high mobility group box protein 1 (HMGB1), interferon type I (IFN I), and heat shock proteins (*e.g.*, Hsp70 & Hsp90) as well as translocation of the endoplasmic reticulum (ER) pro-apoptotic protein, calreticulin (CRT), a crucial “eat me” signal, to the plasma membrane leaflet^{1,6,7}. Consequently, an innate immune response is induced that results in infiltration of phagocytic DCs and macrophages, which enhances the uptake and presentation of dying cancer cell antigens. The matured DCs migrate to lymph nodes, cancer-associated antigenic materials are processed, and naive T cells are primed into effector T cells. Infiltration of these cancer antigen-specific T cells into the tumor promotes immunity *via* release of perforin and granzyme B in addition to secretion of IFN γ and tumor necrosis factor alpha (TNF α) resulting in tumor elimination (Fig. 1)^{8,9}.

Mechanistically, ATP establishes a “find-me” signal that provokes recruitment and activation of antigen presenting cells (APCs) *via* binding to purinergic receptor P2Y (P2RY2) and purinergic receptor P2X (P2RX7). CRT “eat-me/digest” signal binds to low density lipoprotein receptor-related protein 1 (LRP1/CD91) to enhance uptake of antigen by APCs and elicit phagocytosis of dying cancer cells. HMGB1 “danger” signal also binds to and activate toll-like receptor 4 (TLR4) and advanced

glycosylation end product-specific receptor (AGER/RAGE) to promote maturation of DCs and enhance antigen presentation to the CTLs¹⁰. This is associated with cleavage and release of apoptotic cell-associated antigenic fragments in a caspase-dependent manner, which are then transported from phagosomes into cytosolic proteasomes. The cancer-antigenic peptides are then transferred into the ER lumen, where they can bind the appropriate class I molecule¹¹.

ICD can be induced *via* few chemotherapeutics, targeted therapy, radiotherapy, photodynamic therapy (PDT), photothermal therapy (PTT), magnetic hyperthermia, chemodynamic therapy (CDT), sonodynamic therapy (SDT) and oncolytic therapy^{11,12}. Generation of ROS is anticipated to play a key role in ICD induction by establishing stress to ER which in turn help release of DAMPs. Type I ICD inducers, *e.g.*, chemotherapeutics, act mainly by targeting nuclear DNA, cytosolic or plasma membrane proteins as a major focused effect to provoke cell death, while act collaterally by inducing ER stress to release DAMPs. Type II ICD inducers, *e.g.*, hypericin PDT, act selectively on ER to trigger apoptosis and emit DAMPs^{13,14}.

1.3. ICD improves the outcomes of cancer immunotherapy

One of the advantages of ICD, also known as “*in situ* cancer vaccination”, is that the whole tumor-related antigenic repertoire is used, therefore, APC uptake and presentation of a full complement of TAAs is facilitated for both mutagenic and non-mutagenic antigens, which allows for the selection of the most effective T cell receptors (TCRs). This is expected to promote efficient tumor elimination through receptor proofreading^{11,12,15}. Moreover, ICD enables the cognitive immune system to adjust to the constantly changing tumor antigens instead of confining the immune response solely to neo-antigens. On the contrary, traditional vaccines utilize only specific TAAs, incorporating neo-antigens evolving as a result of non-synonymous mutations. These TAAs thus provide limited response and fail to represent diverse scope of cancer cell antigens that may evolve during tumor-induced immune editing. The restricted presentation of antigenic epitopes to the T-cell antigen receptor may lead to an insufficient or ineffective response, as it can easily miss the opportunity to select receptors with favorable on/off binding constants and/or optimal affinity^{16–18}. Mechanistically, the major mechanism of ICD is to enhance the activity of DCs where ICD provides a strong inflammatory response that help trafficking of immune cells to the tumor site and hence triggers T cell immune response against tumor. Thus, ICD is also advantageous to whole-cell cancer vaccines based on using tumor cell lysate prepared by freeze-thawing or irradiation which usually suffers from low activation efficacy of DCs^{15,19}.

1.4. Nanomedicines enhance the efficacy of ICD

Till now, the application of traditional ICD inducers is still limited. In addition to undesirable drug delivery efficiency and off-target toxicity of ICD inducers, the conventional ICD inducing

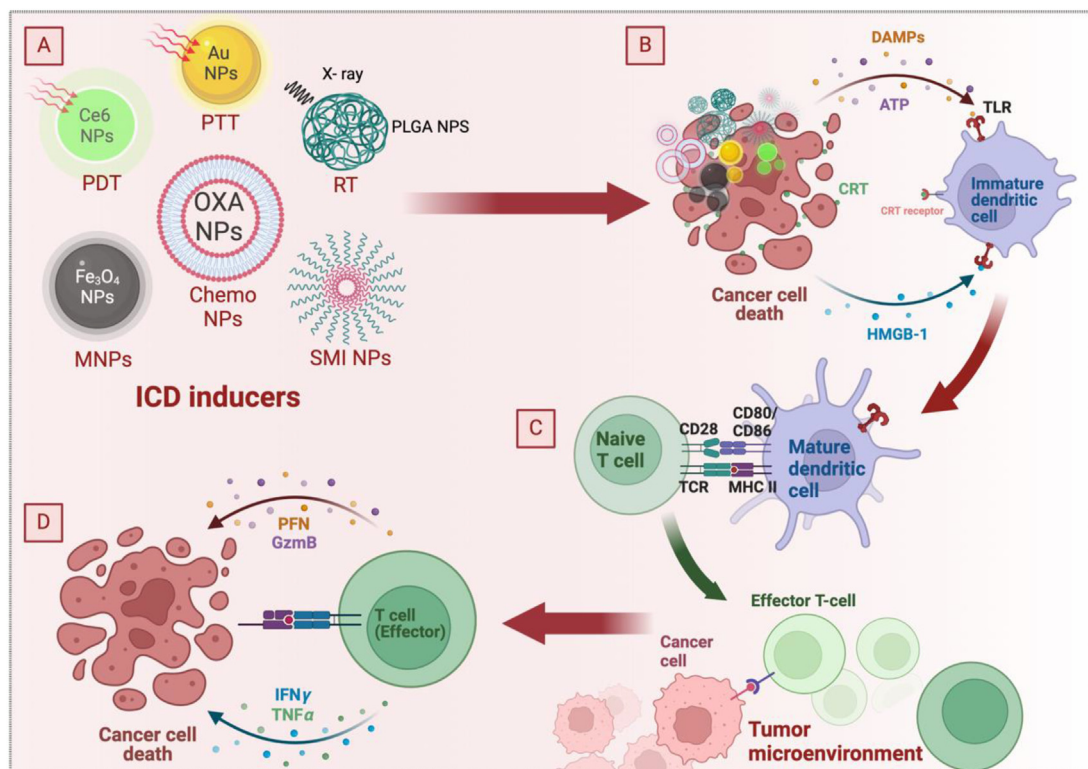


Figure 1 Engineered nanomedicines to trigger immunogenic cell death (ICD) of cancer cells using various approaches. (A) Different types of ICD inducer nanoparticles (NPs) including chemotherapeutic (Chemo NPs), targeted small molecule inhibitors (SMI NPs), photodynamic (PDT), photothermal (PTT), magnetic (MNPs) and radiotherapy (RT) enhancing nanomedicines, can be used to promote the ICD molecular pathway in subsequent steps. (B) The ICD inducer nanomedicines stimulate dying of cancer cells leading to promoted release of TAAs together with DAMPs including extracellular secretion of ATP, HMGB-1, IFN I, as well as surface translocation of the ER protein, CRT⁶. The released DAMPs interact with complementary receptors on APCs to trigger an innate antitumor immunity by recruitment of DCs and macrophages to ICD site and enhance the uptake and presentation of TAAs of dying tumor cells. (C) The matured DCs then reach the lymph nodes to process the TAAs and prime naive T cells into effector CTLs. (D) The tumor antigen-specific T cells will consequently infiltrate the tumor to enhance antitumor immunity *via* release of perforin and granzyme B in addition to secretion of IFN γ and TNF α resulting in tumor elimination (created *via* BioRender).

strategies such as chemotherapeutic drugs and radiotherapy suffer from limited efficacy with relatively weak and transient antitumor immunity after tumor destruction which does not efficiently protect against tumor recurrence^{20,21}. Different forms of nanomedicines were employed to facilitate tumor drug accumulation and deep penetration. This approach aimed to enhance the effectiveness of ICD inducers while minimizing their side effects. Therefore, the use of nanocarriers for selective delivery of ICD-inducing drugs to cancer cells has been reported to boost the therapeutic outcomes in animal tumor models and show synergistic activity with different modalities of immunotherapy (Table 1)^{22–31}.

2. ICD inducing nanomedicines

2.1. Chemotherapeutic nanomedicines

Some of chemotherapeutic drugs were reported to elicit an antitumor immune response. However, some challenges limit their use including; i) inefficient tumoral drug accumulation resulting in weak apoptosis and moderate antitumor immune response, and ii) severe systematic and immune toxicities^{13,32}. Therefore, loading of those drugs into nanocarriers increases their tumor accumulation and hence reduces their systemic

toxicity and enhances their efficacy resulting in sufficient induction of ICD anti-tumor immune response^{1,33}.

2.1.1. Doxorubicin (DOX)

Low dose of DOX was found to induce ICD of cancer cells associated with expression of DAMPs including CRT, HMGB1, and Hsp70 with reduction of the dose-relevant cytotoxicity^{34,35}. DOX-carrying high-density lipoprotein-mimicking nanodiscs (sHDL) were formulated by mixing acid responsive phospholipid-DOX conjugate with apolipoprotein A1 mimetic peptide³⁵. The ultrasmall size (10 nm) and long systemic circulation of sHDL enhanced tumor accumulation of DOX and increased its uptake into cancer cells due to their need for high level of lipids and cholesterol for growth. The released DOX triggered ICD thus induced efficient antitumor CD8⁺ T cell-based immunity that could potentiate immune checkpoint blockade by α PD-1 antibodies resulting in tumor elimination in CT26 and MC38 colon carcinoma bearing mice³⁵. Similarly, single intravenous administration of chimeric polypeptide DOX conjugate NPs stimulated an antitumor immune response in poorly immunogenic 4T1 mammary carcinoma bearing mice³⁶. This was evidenced by increased secretion of chemokines CCL2–5 and CXCL10 and infiltration of CTLs into tumor as well as repolarization of the immunosuppressive tumor-supportive MDSCs to anti-tumor phenotype.

Table 1 Selected examples of ICD inducer nanomedicines and synergistic modalities.

Particle material	ICD inducer	ICD induction mechanism & cellular target	Synergistic combined modality	<i>In vitro</i> cancer cell line	<i>In vivo</i> tumor model	Ref.
Self-assembled PEGylated lipid binary NPs	Oxaliplatin (OXA)	Chemotherapy DNA synthesis	NLG919 (IDO-1 inhibitor)	4T1 breast cancer cells	Orthotopic 4T1 breast & subcutaneous CT26 colorectal tumor models	23
Hyaluronic acid conjugated polylysine NPs	Chlorin e6 (Ce6)	Photodynamic therapy (PDT) ER stress (ROS)	1-MT (IDO-1 inhibitor) & aPD-L1	B16F10 melanoma cells	Bilateral B16F10 melanoma primary model & lung metastasis model	24
Polypyrrole nanosheets	Polypyrrole AuNPs	Photothermal therapy (PTT)	aPD-L1	4T1 breast cancer cells	Subcutaneous 4T1 breast tumor model	25
CoFe ₂ O ₄ @MnFe ₂ O ₄ NPs	CoFe ₂ O ₄ @MnFe ₂ O ₄ NPs	Magnetic hyperthermia	aPD-L1	4T1 breast cancer cells, U87 brain astroblastoma cells	Bilateral subcutaneous 4T1 tumor model	26
Mannosylated lactoferrin NPs	Shikonin (SHK)	PKM2 protein, 20S subunit of proteasome	JQ1 (PD-L1 suppressor)	CT26 cells	Subcutaneous CT-26 murine colorectal model	27
PLGA core-shell NPs	X-ray radiation	Radiotherapy (RT) DNA strand breaks	Catalase, Imiquimod (TLR7 agonist), CTLA-4 antibody	4T1 breast cancer cells, CT26 colon colorectal cells	Orthotopic 4T1 breast metastasis model & subcutaneous CT26 colorectal tumor model	28
Manganese zinc sulfide NPs copolymer micelles	ZMS NPs IR780	Chemo-dynamic therapy (CDT) & PTT	IR780 (PTT dye)	B16F10 melanoma cells	B16F10 melanoma tumor model	29
Semiconducting polymeric NPs	PFODBT	Sonodynamic therapy (SDT)	Tirapazamine (cytotoxic), Ibrutinib (MDSC inhibitor)	4T1 cells	4T1 primary and lung metastasis tumor models	30
Chimeric polymersomes	LTX-315 (LTX)	Oncolytic therapy Mitochondria permeabilization	CpG, (TLR9 agonist), aPD-L1	B16F10 melanoma cells	B16F10 melanoma tumor model	31

OXA: oxaliplatin; 1-MT: dextro-1-methyl tryptophan; PKM2: pyruvate kinase M2; PLGA: poly(lactic-co-glycolic) acid; ZMS NPs: manganese zinc sulfide NPs; PFODBT: poly[2,7-(9,9-di-octyl-fluorene)-alt-4,7-bis(thiophen-2-yl)benzo-2,1,3-thiadiazole]; CpG: cytosine-phosphate-guanine oligonucleotides.

2.1.2. Oxaliplatin (OXA)

OXA is a promising third-generation platinum drug with similar anticancer effect to cisplatin but without its toxic effects. It exerts its activity by inducing DNA damage, providing ribosome biogenesis stress and by triggering ICD by release of DAMPs and ROS. However, its repeated use can cause neurotoxicity and renal failure⁹. Loading of OXA into amphiphilic PEGylated poly(lactic-co-glycolic) nanoparticles (PLGA NPs) could release more DAMPs and hence more efficiently induced ICD and triggered greater maturation of DCs and infiltration of T cells compared to free OXA treatment in Pan02 pancreatic cancer bearing mice⁹. Another platinum drug, diaminocyclohexane-platinum (DichtPt) was loaded into CD44-targeted hyaluronate-polyarginine electrostatic nanocomplex resulting in higher cytotoxicity to HT-29 and B6KPC3 cells than free OXA³⁷. In addition to its direct cytotoxicity to B6KPC3 pancreatic cancer cells, the NPs elicited antitumor immune response with release of HMGB1 and ATP.

2.1.3. Mitoxantrone (MTX)

Cancer cells can evade the immune response to the vaccines that use specific tumor antigens by downregulating that antigen. To overcome this challenge, ICD could be utilized to develop whole cancer cell vaccine by using immunogenically dying cancer cells treated or surface-decorated with adjuvant-encapsulated NPs³⁸. This enables eliciting an immune response against wide repertoire of tumor antigens released by patient's tumor cells. Therefore, B16F10OVA melanoma cells expressing ovalbumin (OVA), were treated with MTX for 12 h to induce ICD. Maleimide-derivatized CpG-loaded cationic liposomes/hyaluronate hybrid NPs were then coupled to those immunogenically dying melanoma cells *via* their membrane free sulfhydryl groups. Compared to live tumor cells, MTX-treated tumor cell-CpG-NP conjugates were 4.2-fold more remarkably phagocytosed by DCs. Surface modification of cells with CpG-NPs has enhanced the cross-presentation of OVA protein, increased expression of CD40 and CD86 on DCs, and increased the secretion of IL-12p70, TNF- α , and IFN- β from DCs³⁸. In an animal model, a single subcutaneous dose of MTX-treated B16F10OVA cells/CpG-NP conjugate induced a potent antigen-specific CD8 α^+ T cell response. This effectively protected all mice from the onset of tumors.

2.2. Radiotherapy enhancing nanomedicines

Radiotherapy (RT) is another method that aims to destroy DNA double strands in order to treat local solid tumors. In recent years, RT was shown to induce a systemic immune response. This response has been observed to affect remotely located tumor deposits, even those not directly exposed to radiation, through a phenomenon known as abscopal effect^{39,40}. Mechanistically, RT uses X-rays to generate hydroxyl radical ($\cdot\text{OH}$) to induce damage of the tumor cellular components, including DNA, proteins, and membranes. It was repeatedly shown that RT triggers antitumor immune responses by exposing CRT, and *via* the induction of the release of TAAs, Hsp70 and HMGB1. This result suggests that RT induces ICD *in situ*, while stimulating the maturation of DCs and induction of IFN γ -producing T cells both *in vitro* and *in vivo*. The efficacy of RT was significantly enhanced when combined with PLGA NPs encapsulating catalase and a potent TLR-7 agonist, imiquimod²⁸. Catalase acts by decomposing H₂O₂ into H₂O and O₂, which reduces hypoxia-accompanied resistance to radiotherapy while imiquimod acts by reversing the immunosuppressive TME. This

combination enhanced the destructive power of X-ray RT against primary CT26 murine tumor, where the NPs triggered ICD as shown by translocation of CRT and enhanced maturation of DCs²⁸.

2.3. ICD targeted SMI nanomedicines

A number of small molecule inhibitors (SMIs) of major signaling pathways were found to trigger various forms of apoptosis, including ICD which elicits antitumor immune response. The proteasome inhibitor bortezomib (BTZ)⁴¹, tyrosine kinase inhibitor crizotinib^{42,43}, multi-kinase inhibitor, regorafenib^{44,45}, and pyruvate kinase M2 (PKM2) inhibitor shikonin (SHK)^{46,47}, are among ICD inducers^{48,49}. BTZ was shown to trigger Hsp90 and CRT expression by human or mouse multiple myeloma (MM) cells thus enabling their recognition and phagocytosis by DCs⁵⁰. Incorporation of BTZ into pH-responsive polyhyalazine NPs enhanced its accumulation in tumors⁵¹. The release of the vasodilator drug hyalazine resulted in dilating tumor blood vessels which remodeled TME and alleviated hypoxia. The NPs induced ICD, thereby enhancing the infiltration of CTLs in tumors compared with free BTZ treatment leading to significantly reduced tumor growth, and suppressed lung metastasis.

Crizotinib, in high dose (≥ 10 $\mu\text{mol/L}$), was able to trigger ICD of lung adenocarcinoma and skin fibrosarcoma cells that lack mutations of ALK and ROS1 *via* "off-target" mechanism. As a result, the combined use of crizotinib with non-ICD inducer drug cisplatin synergistically suppressed the growth of orthotopic non-small cell lung cancer (NSCLC) mouse model and boosted the efficacy of anti-PD-1 antibody⁴². Recently, low dose crizotinib (≤ 5 $\mu\text{mol/L}$) also induced ICD in anaplastic large cell lymphoma showing ALK mutation *via* "on target effect" as demonstrated by excessive CRT exposure as well as release of ATP and HMGB1^{43,52}. Crizotinib has also been reported to specifically inhibit the c-Met pathway which can synergistically boost the chemotherapy-induced ICD. Therefore, polymerized crizotinib prodrug was synthesized and self-assembled into micelles for DOX encapsulation⁵³. The DOX/crizotinib micelles synergistically enhanced the tumoral infiltration of CTLs, reduced the immunosuppressive Treg cells, accompanied with the increased cytokine secretion of IFN- γ and TNF- α , leading to suppression of tumor growth in 4T1 breast cancer mice. Regorafenib was also reported to enhance ICD of triple negative breast cancer cells *via* STAT3 suppression. Oral administration of regorafenib into 4T1 syngeneic mouse model resulted in overexpression of CRT and HMGB1 with a consequently increased intratumoral infiltration of CD8 $^+$ and CD4 $^+$ T cells and enhanced maturation of DCs⁴⁴.

Shikonin (SHK), a PKM2 inhibitor with antitumor efficiency, is also known to induce ICD through binding and interfering with its heterogeneous nuclear ribonucleoprotein A1 (hnRNP A1), triggering necroptosis and ROS generation thus eliciting antitumor immunity and promoting DC maturation⁵⁴. Therefore, SHK was encapsulated into various types of nanomedicines to enhance ICD power (Fig. 2). Encapsulation of SHK into lactoferrin NPs amplified its ICD power showing highest immunogenicity as demonstrated by high level (83%) of CD80 $^+$ CD86 $^+$ mature DCs, increased tumor infiltrating CD8 $^+$ T cells and reduced infiltration of Tregs compared to free SHK²⁷. Those effects could be mediated through remarkable increase of surface exposure of CRT and release of HMGB1 from CT26 cells. SHK was co-encapsulated with other immune

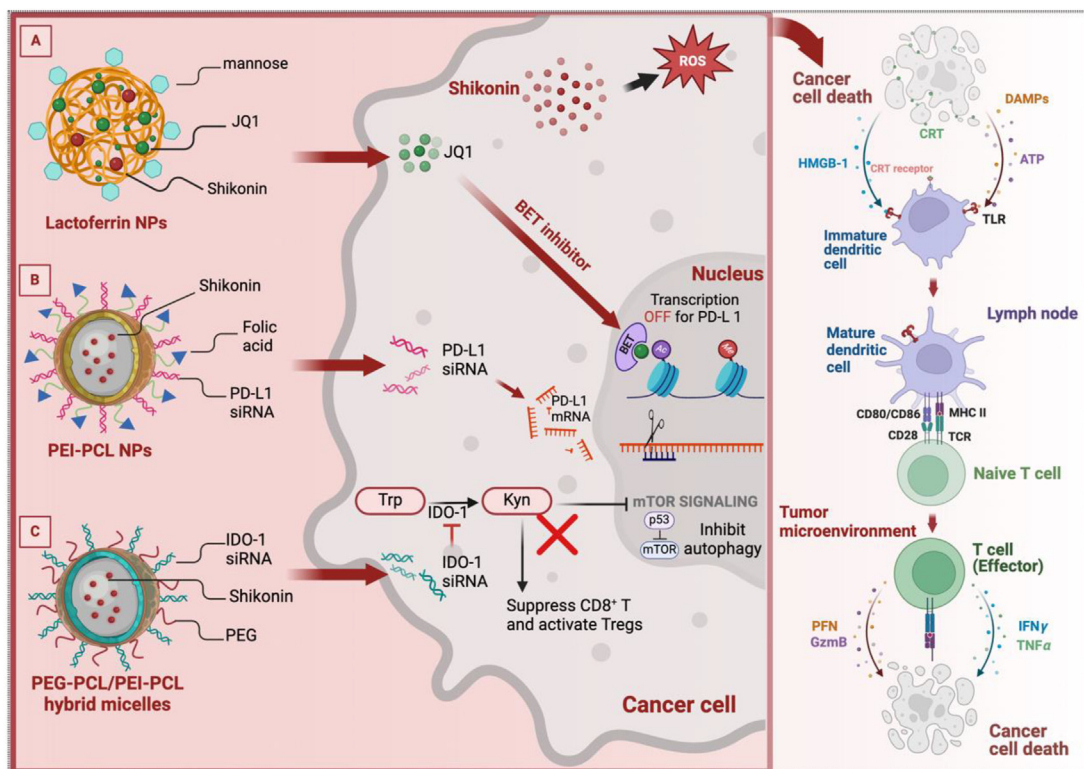


Figure 2 Shikonin (SHK) ICD inducer nanomedicines. (A) Mannosylated lactoferrin NPs where SHK was co-encapsulated with JQ1, a bromodomain and extra-terminal motif (BET) inhibitor²⁷. (B) Polyethyleneimine-polycaprolactone (PEI-PCL) NPs where SHK was co-encapsulated with PD-L1 siRNA⁵⁵, and (C) hybrid PEGylated polycaprolactone (PEG-PCL) micelles where SHK was co-loaded with IDO-1 siRNA⁵⁶ (created *via* BioRender).

checkpoint inhibitors (PD-L1 siRNA) or immunomodulators (IDO-1 siRNA) *via* NPs and hybrid micelles, respectively^{55,56}. Both systems successfully boosted the antitumor immune response and reversed the immunosuppressive TME.

2.4. Photodynamic nanomedicines

Photodynamic therapy (PDT) has been proposed as a novel noninvasive and target-specific anticancer therapeutic approach. Upon exposure to light, photosensitizers (PSs) convert the oxygen nearby into harmful ROS such as singlet oxygen ($^1\text{O}_2$), which induces apoptotic and necrotic cell death. Moreover, PDT-induced cell death results in release of DAMPs including surface expression of CRT, secreted ATP and HMGB1⁵⁷. PDT has also been found to induce an up-regulation of the transcription factor nuclear factor kappa B (NF- κ B) and Hsp70, activating DCs which further stimulate the host antitumor immune response. Typically, PSs are hydrophobic molecules that tend to aggregate in aqueous media, which could reduce $^1\text{O}_2$ formation, and thus cause insufficient tumor localization⁵⁸. Hence, targeted delivery of PSs to tumors using NPs, combined with precise control over light exposure, aims to decrease the systemic toxicity caused by PSs. Chimeric peptide NPs were synthesized by encapsulating the PS protoporphyrin IX (PpIX) with 1-methyltryptophan (1MT) as IDO inhibitor⁵⁹. Upon light irradiation, the PpIX-1MT NPs triggered apoptosis in CT26 colon adenocarcinoma, mediated *via* facilitated expression of caspase-3 and production of TAAs. Subsequently, the released 1MT stimulated CD8⁺ T cells by suppressing the

IDO pathway. This combined action acted synergistically to suppress both primary tumor and lung metastasis⁵⁹.

2.5. Photothermal nanomedicines

Photothermal therapy (PTT) is used as a noninvasive cancer therapeutic strategy that acts by two mechanisms; direct killing of tumor cells *via* light-induced hyperthermia and indirectly by triggering adaptive immune response. PTT is based on the intrinsic capacity of light-absorbing inorganic agents (*e.g.*, Au NPs, Pd NPs, CuS NPs, GO, MoS₂ nanosheets, or carbon nanotubes) to convert photoenergy into heat. The generated temperature increase kills cancer cells by damaging the cell membrane, causing protein denaturation, and triggering DNA damage. Moreover, hyperthermia causes the ablated tumor cell residues to release TAAs, DAMPs and Hsps which further improve ICD efficacy. Prussian blue NPs were reported to effectively induce ICD in neuroblastoma cells *via* PTT effect with an optimal thermal window of 63.3–66.4 °C for the highest expression of DAMPs⁶⁰. The *in vivo* administration of the NPs into neuroblastoma mouse model within the optimal thermal window induced survival of 33.3% of mice for 100 days. In a similar vein, Yu and colleagues⁶¹ indicated that the PTT effect generated by AuNPs can stimulate an increase in Hsp70 expression in colorectal cancer cells.

Recently, conductive polymer NPs fabricated from polypyrrole and polyaniline were explored for PTT ablation⁶². Under 808 nm laser irradiation, the NPs composed of poly(3,4-ethylenedioxythiophene) (PEDOT) exhibited powerful absorption of light between 700 and

900 nm resulting in a temperature rise of about 32 °C which induced death of MDA-MB-231 cells after 5–15 min of laser irradiation. Upon NIR laser irradiation, the cells were killed along with release of DAMPs mainly *via* apoptosis after exposure to the PEDOT NPs for 1.5, 6, and 12 h, while longer exposure times resulted in cell necrosis⁶². Development of particles that absorb in the second near-infrared region (NIR-II) marks a significant leap forward for PTT due to their improved tissue penetration⁶³. The NPs based on diammonium polymer, exhibited heightened absorption within the 1000–1100 nm range, and demonstrated impressive PTT conversion efficiency of 34.7%⁶⁴. The NPs showed formidable PTT activity leading to complete eradication of tumors in a 4T1 tumor mouse model along with generating ICD-immune response.

Compared to the commonly used continuous-wave laser system, pulsed-wave (PW) laser involves irradiation of cancer cells with short pulses that ablate tumor by a combined PTT and photomechanical effect termed photothermolysis⁶⁵. The PW laser offers better control in inducing cell death and higher penetration depth than continuous-wave laser. Under irradiation with 15 ns laser pulses, copper sulfide (CuS) NPs-mediated photothermolysis enhanced intratumoral infiltration of DCs and CTLs in B16-OVA mouse model. In combination with poly(L-glutamic acid)-CpG conjugate and α PD-1, CuS NPs markedly enhanced survival of mice re-challenged with tumor cells at a distant site in the poorly immunogenic ovarian tumor model *via* abscopal effect⁶⁵.

2.6. Magnetic nanomedicines

Magnetic nanoparticles (MNPs) are capable of converting an external alternating magnetic field (AMF) into heat *via* a hysteresis process. Compared to PTT therapy (above 50 °C), magnetic hyperthermia is safe where the magnetic NPs generate mild hyperthermia with a temperature below 44 °C within the tumor tissue, thereby selectively killing the tumor cells^{66,67}. In contrast, photobleaching and phototoxicity are major safety limitations for high-light dose phototherapy. More importantly, while light cannot reach distant cancer metastatic sites, the magnetic field has higher tissue penetration⁶⁸. In addition, ferroptosis was reported as an iron- and ROS-dependent form of apoptosis. Ferroptotic agents can trigger an unfolded protein response which contributes to ER stress^{69,70}.

Superparamagnetic NPs were also developed to generate magnetic hyperthermia that induces ICD of cancer cells based on mitochondrial heat stress rather than the traditional ER stress-based ICD⁷¹. To enable tumoral mitochondrial targeting, the NPs were modified with RGD and (3-carboxypropyl)triphenylphosphonium bromide (TPP). Such a mitochondrial heat stress resulted in intramitochondrial ROS generation and ICD of Hepa 1–6 hepatoma cells under AMF. Moreover, the heat stress-induced damage of mitochondria further induced ER stress by down-regulating mitofusin 2 at mitochondria-associated membranes (MAMs) *via* PERK/eIF2 α pathway. This resulted in release of DAMPs including CRT, ATP and Hsp70 which repolarized M2 macrophages into anti-tumor M1 phenotype and increased its phagocytic activity against cancer cells.

Innovative approaches have been introduced to overcome the limitations of traditional superparamagnetic iron oxide NPs (SPIONs), such as low conversion efficiencies. Among these novel strategies, ferrimagnetic vortex-domain iron oxide nanorings (FVIOs) enable an exceptionally high specific absorption rate of over 3000 W/g which is a tenfold increase compared to U.S. Food and Drug Administration (FDA)-approved iron oxide NPs like

ferumoxytol⁷². Biocompatible FVIOs coated a dense polymer shell of 4arm-PEG-NH₂ have been designed as efficient nanomediators that generate moderate heat within the tumor site under AMF through a vortex-to-onion magnetization reversal process. In this way, FVIOs exhibit superior magnetic thermal behavior while simultaneously ensuring improved colloidal stability, good suspension and rapid magnetic response. FVIO-mediated mild magnetic hyperthermia triggers apoptosis and CRT exposure on 4T1 breast cancer cells, thereby enhancing phagocytic uptake of cancer cells and triggering powerful ICD. This mild thermotherapy induced an 88% enhancement in CTL infiltration in distant tumors and sensitized tumors to PD-L1 checkpoint blockade, thereby hindering lung metastasis⁷².

2.7. Chemodynamic nanomedicines

Chemodynamic therapy (CDT) is an innovative approach that induces ICD of cancer cells by utilizing transition metal ions, typically iron or manganese, to catalyze Fenton or Fenton-like reactions. These reactions generate highly reactive hydroxyl radicals (\cdot OH), among the most toxic forms of ROS, from H₂O₂ in the TME resulting in strong oxidative stress⁷³. CDT could be mediated under AMF using magnetic iron oxide NPs *via* Fenton-like reaction⁶¹. The MNPs augmented the anti-tumor response by initiating ICD, evident from the increased expression of HMGB1 and CRT as well as increased tumor-infiltrating CD8⁺ T resulting in suppressed tumor growth in melanoma bearing mice. In another study, manganese zinc sulfide NPs (ZMS NPs) were combined with the dye IR780 *via* thermally responsive copolymer micelles to amplify the combined PTT/CDT-mediated ICD response²⁹. Under NIR irradiation, ZMS NPs were released and provided high level of Mn²⁺-triggered hydroxyl radicals (\cdot OH) produced *via* Fenton-like reaction resulting in ICD-related DAMPs exposure. Moreover, as an immune adjuvant, the released Mn²⁺ enhanced the sensitivity of dsDNA recognition by the cGAS-STING signaling leading to producing type I interferon (particularly IFN- β), which can enhance the immune response in metastatic melanoma²⁹. Synergistically, IR780 accumulated within the mitochondria of cancer cells, thereby augmenting PTT destruction and increasing accumulation of DAMPs leading to further activation of DCs in B16F10 melanoma tumor bearing mice.

2.8. Sonodynamic nanomedicines

Sonodynamic therapy (SDT) can induce ICD of cancer cells by selectively activating sonosensitizers under US to generate ROS in addition to the cavitation mechanism. SDT offers a safe and noninvasive localized approach with minor damage to normal tissues and higher ability to penetrate deep distant tumors compared to PDT and PTT⁷⁴. However, the increased oxygen depletion during SDT results in hypoxia and recruitment of immunosuppressive MDSCs⁷⁵. A combined ferroptosis/SDT approach was used to overcome the hypoxia of the solid tumors, consequently improving the SDT efficiency. Ferroptosis results in glutathione depletion and accumulation of lipid peroxides which enhance the oxidative stress and release of DAMPs⁷⁶. Therefore, hemoglobin liposomes were combined with SDT to promote ICD *via* promoting ferroptosis and generating lipid-reactive oxide species during the SDT⁷⁷. The liposomes also enhanced α PD1 therapy resulting in superior inhibition of colon CT26 tumor-bearing mice. In another investigation, sono-activatable semi-conducting polymeric NPs were developed for US-responsive

release of tirapazamine (TPZ) and ibrutinib (IBT)³⁰. After accumulation into tumor sites, the generated $^1\text{O}_2$ via SDT effect under US treatment resulted in ICD of 4T1 cells. Meanwhile, TPZ was activated to toxic form only at the hypoxic tumor which strengthened the ICD response while IBT inhibited the immunosuppressive activity of MDSCs to enhance the antitumor immune response. The NPs inhibited the growth of primary 4T1 tumors and suppressed the growth of distant tumors and tumor metastasis in lungs and livers. The ROS-generating sonosensitizer IR780 and the oxygen-carrying perfluorohexane co-loaded into PEGylated PLGA NPs showed powerful ICD effect on ID8 ovarian cancer cells and mouse model under US stimulation⁷⁸. US irradiation of temozolomide-loaded liposomes generated high amount of ROS with sonotoxic effect to LN229 and GL261 glioma cells⁷⁹. This response was associated with enhanced release of DAMPs such as CRT and HMGB1 and maturation of DCs with suppressed growth of GL261 mouse orthotopic glioma model.

2.9. Oncolytic nanomedicines

Oncolytic peptides demonstrate a high degree of efficacy in altering the TME and enhancing anticancer immune responses. This is achieved through various mechanisms, notably by triggering ICD⁸⁰. The amphipathic cationic oncolytic peptide LTX-315 was found to promote the release of DAMPs including HMGB1 and chemokine CXCL10 *via* a different mechanism than chemotherapeutics. The peptide induces pore formation in cancer cell membrane in addition to disintegrating the cytoplasm and mitochondria⁸¹. As a result, LTX-315 could rapidly reprogram the TME by decreasing the infiltration of Tregs and MDSCs while increasing the infiltration of T helper and cytotoxic T cells. However, LTX-315 is only used by intratumoral injection for treatment of accessible tumors such as melanoma. To enable its systemic delivery, cRGD-functionalized chimeric polymersomes encapsulating LTX-315 were developed³¹. The use of LTX-NPs in combination with CpG adjuvant and anti-PD-1 induced strong apoptosis (63.3%) of B16F10 cells with enhanced release of DAMPs and increased the mitochondria permeability with release of apoptotic effectors. In B16F10 melanoma bearing mice, the LTX combined therapy enhanced infiltration of CD8⁺ CTLs and helper T cells, in addition to reduction of Tregs. Moreover, the combination resulted in generating long-term immune memory which enabled resistance to re-challenged B16F10 cells compared to mice treated with free LTX-315 which developed tumor relapse. In another approach, cRGD-coupled polymer-lipid hybrid NPs co-delivering LTX-315 peptide and TGF- β 1 siRNA were designed⁸². The released DAMPs were enhanced in LTX NP-treated 4T1 tumor cells including translocation of CRT, and the release of ATP and HMGB1. Treatment of BMDCs with the supernatant from NP-treated 4T1 cells resulted in DC activation with upregulation of CD80 and CD86. After intravenously injected into mice, the hybrid NPs could effectively extend the half-life of LTX-315 peptide. In combination with NKG2A checkpoint inhibitor therapy, the NPs increased infiltration of CD8⁺NKG2D⁺ and NK1.1⁺NKG2D⁺ cells, inhibited the tumor growth and prolonged survival rate of treated mice.

In addition to oncolytic peptides, oncolytic viruses (OVs) have been reported to induce tumor lysis, and trigger ICD *via* intratumoral administration⁸³. However, the low efficiency of OVs monotherapy, and inaccessible intratumoral administration limit their application. Lung cancer cell-derived extracellular vesicles (EVs) 50–400 nm were isolated from LL/2 mouse lung cancer

cells and co-loaded with PTX and oncolytic adenovirus (Fig. 3)⁸⁴. The selective tumor homing of EVs due to expressing tetraspanins and integrins enhanced their cancer cell internalization and protected the virus from the host immune-surveillance. The OV-PTX co-loaded EVs triggered the highest ICD of cancer cells as revealed by higher CRT cell exposure and released ATP compared to monotherapy resulting in enhanced tumoral infiltration of CTLs and improved anti-tumor effects in LL/2 lung cancer-bearing mice⁸⁴.

3. Multi-modality ICD nanomedicines

Single ICD inducers usually fail to trigger ER stress sufficient to elicit powerful ICD and efficient antitumor immune response. Multimodality combination NPs can combine multiple therapeutic agents or modalities to increase the response rate of ICD inducers and overcome immune evasion.

3.1. Combined chemotherapy-induced ICD

3.1.1. Chemo/targeted SMI therapy

SHK was combined with MTX or DOX to synthesize dual-loaded liposomes to trigger a synergistic ICD-mediated cytotoxic killing of cancer cells⁸⁵. The dual-loaded liposomes triggered efficient antitumor immunity at lower drug doses which can also reduce the toxicity of both drugs. Celestrol (CEL) has also been found to facilitate ICD by inducing ER stress *via* promoting calcium release from ER and mitochondria leading to ER accumulation of mis-folded proteins and impaired activities of chaperones (*e.g.*, Hsp90) resulting in cell apoptosis and release of TAAAs⁸⁶. Therefore, MTX and CEL were co-loaded in anisamide-modified NPs that selectively bind to sigma receptors over-expressed on both melanoma and cancer associated fibroblasts. The strong synergy between MTX and CEL effectively promoting ICD has resulted in surface expression of CRT by cancer cells, with enhanced secretion of HMGB1 as standard markers for drug-induced tumor cell immunogenicity⁸⁶.

3.1.2. Chemotherapy/PDT

Chemotherapy-induced ICD is usually insufficient to trigger antitumor immune response since they only exert secondary ER stress. Therefore, combination with PDT which focuses on inducing ER stress *via* ROS generation is anticipated to produce synergistic ICD response. Core-shell NPs were developed by polymerization of Zn²⁺ oxaliplatin (OXA) coordinate in the core while coated with PEGylated shell contains photosensitizer pyropheophorbide-lipid ester bond-based conjugate (pyrolipid)⁸⁷. Injection of CT26 cells pre-treated with the NPs under light-irradiation to undergo ICD into mice successfully prevented tumor development after re-challenging with live tumor cells. When combined with PD-L1 blockade, the NPs suppressed the growth of both irradiated primary tumor and non-irradiated distant tumor in CT26 and MC38 tumor models *via* the abscopal effect through generating systemic antitumor T-cell immune response⁸⁷.

3.1.3. Chemotherapy/PTT

Inducing ICD, particularly in remote and deeply located tumors remains a formidable challenge. A multimodality combination nanomedicine was developed for co-delivery of DOX and the PTT palladium NPs (Pd NPs) by encapsulation into amphiphile triglycerol monostearates (TGMs)²⁰. Within TME, the lipid ester in

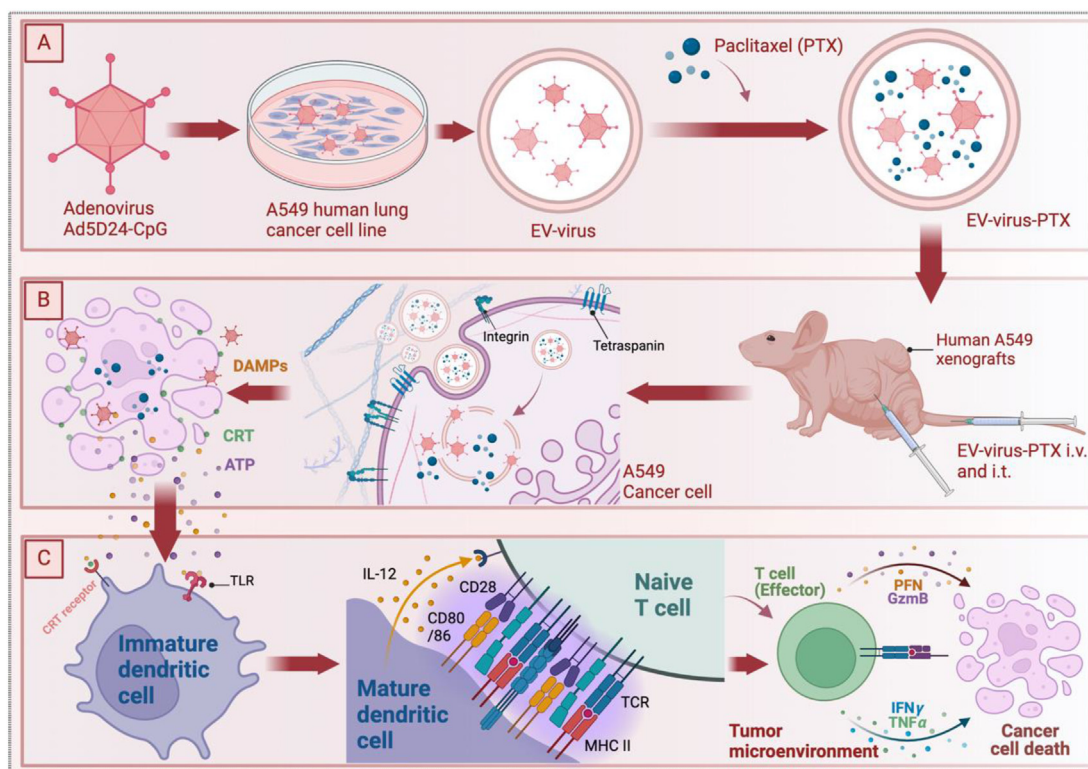


Figure 3 Combined chemotherapy/oncolytic virus (OV)-loaded extracellular vesicles (EVs) approach to trigger ICD effect. (A) Lung cancer cell-derived EVs were isolated from lung cancer bearing mouse and co-loaded with PTX and oncolytic adenovirus. (B) Selective tumor homing of the EVs, enhanced their cancer cell internalization, and consequently induced ICD of cancer cells. (C) These events lead to DC maturation, T cell priming and increased tumoral infiltration of T-cells resulting in enhanced anti-tumor effects in lung cancer bearing mice⁸⁴ (created *via* BioRender).

the TGM structure could be hydrolyzed by the over-expressed matrix metalloproteinase 2 (MMP2) and esterase. When exposed to 808 nm laser irradiation for 10 min, the temperature of Pd-DOX NPs quickly rose within 6 min, reaching 50 °C above the tumor ablation temperature of 42 °C. This elevated temperature is sufficient to trigger apoptosis in tumor cells along with enhanced ICD and release of ATP, HMGB1 and CRT molecules thus increasing maturation of DCs and infiltration of T cells in CT26 tumor-bearing mice²⁰. The OXA-induced ICD may not result in a robust antitumor immune response due to insufficient Pt-DNA crosslinks. Recently, polymeric NPs co-loaded with a platinum (IV) prodrug of OXA (Pt(IV)-C16) and a NIR-II PTT agent IR1061 were developed to enhance OXA-induced ICD⁸⁸. Upon irradiation with NIR-II light, the generated mild hyperthermia was found to augment the OXA-mediated ICD by increasing the Pt-DNA crosslinking resulting in enhanced DNA damage and apoptosis. As a result, the NPs efficiently suppressed the tumor growth in 4T1 tumor-bearing mice with increased expression of CRT in tumor tissues and consequently enhanced infiltration of CD4⁺ and CD8⁺ T cells.

3.1.4. Chemotherapy/magnetic NPs

To improve the ICD efficacy of OXA, core-shell magnetic NPs with Fe₃O₄ core were used to release ferric ions that can promote the OXA-induced ICD. Modifying the OXA containing polymeric shell of NPs with α -enolase targeting peptide (ETP) enhanced their cellular internalization into 4T1 cancer cells *via* binding to α -Enolase, a plasminogen-binding receptor, over-expressed on

cancer cell surface⁸⁹. The internalized OXA can produce intracellular H₂O₂, *via* nicotinamide adenine dinucleotide phosphate oxidase (NOX) stimulation and superoxide dismutase (SOD)-mediated superoxide anion (O₂^{•-}) dismutation leading to DNA lesions and ROS generation. Simultaneously, the generated H₂O₂ can be utilized by the released ferric ions through Fenton's reaction to induce the release of highly toxic ROS (\cdot OH or \cdot OOH) resulting in RE stress which boosts the ICD-associated immunogenicity⁸⁹.

3.2. Combined phototherapy-induced ICD

3.2.1. Combined PDT/PTT

PDT and PTT can be combined together to enable synergistic phototherapy for enhancing ICD efficacy. Novel NPs were developed with polydopamine (PDA) core, a PTT agent with powerful NIR absorption and coated with a shell of NaGdF₄:Yb/Er upconversion NPs (UCNPs)⁹⁰. The photosensitizer, Ce6 with its absorption largely overlaps with the emission spectrum of PDA-UCNPs, was further loaded to the surface of NPs to provide PDT. The outer shell maximized their photoabsorption resulting in enhanced ROS generation for PDT after irradiation and preserved the PTT effect of PDA core. The prepared NPs demonstrated high ability of PTT conversion and upconversion emission enabled by both direct absorption of 980 nm laser irradiation and visible emission through UCNPs. Therefore, the light irradiated NPs triggered ICD with CRT exposure onto the membrane of 4T1 cells leading to enhanced intratumoral infiltration of CTLs, B cells and

macrophages⁹⁰. The synergistic phototherapy combined with PD-L1 antibodies could eliminate the tumors after NIR irradiation in 4T1 tumor-bearing mice and effectively inhibited the growth and spread of 4T1 and B10F16 cells in tumor metastasis models.

3.2.2. PDT/magnetic hyperthermia

Since PDT efficacy is hampered by the hypoxia due to excessive oxygen consumption, magnetic hyperthermia can be combined with PDT to increase the tumor oxygen levels and hence may have synergistic antitumor efficacy⁹¹. However, the efficiency of this approach against deep and metastatic tumors is very limited due to the weak penetration capacity of the excitation light. Therefore, Janus nanobullets composed of magnetic Fe₃O₄ NPs anchored onto disulfide-bridged mesoporous silica NPs (M-MSNs) loaded with Ce6 in its pores were synthesized for combined PDT, magnetic hyperthermia and MRI⁹². In reductive GSH tumor conditions, the disulfide bonds in the structure of the M-MSNs were cleaved and Ce6 was released due to the matrix degradation of the silica. PDT and magnetic hyperthermia triggered ICD, resulting in surface CRT expression and HMGB1 secretion. Moreover, the NPs successfully suppressed the growth of orthotropic MCF-7 and 4T1 tumors in mice.

4. Synergistic ICD approaches

Despite the important benefits gained by ICD through releasing tumor antigens to act as *in situ* vaccines which activates DCs and initiate the anti-tumor immune response, the immunosuppressive TME generated by suppressive immune cells, enzymes and cytokines counteract both DC maturation and T cell activation. Therefore, multiple immunomodulator therapies were combined with ICD inducer nanomedicines to relieve immunosuppression. We highlight the various synergistic nanomedicines designed to boost the ICD antitumor immunity.

4.1. Immune checkpoint modulators

4.1.1. PD-1/PD-L1 blockade

Self-assembled core shell NPs were synthesized to carry OXA-Zn coordinate polymerized prodrug in the DOPA lipid core, and were coated by a PEGylated lipid bilayer incorporating a cholesterol-disulfide bridge-dihydroartemisinin (DHA) conjugate (chol-DHA)⁸. Once inside the cells, the cytoplasmic reducing environment disrupts the core-shell structure and expose the OXA core and chol-DHA (Fig. 4A). The combined ROS generation capacity

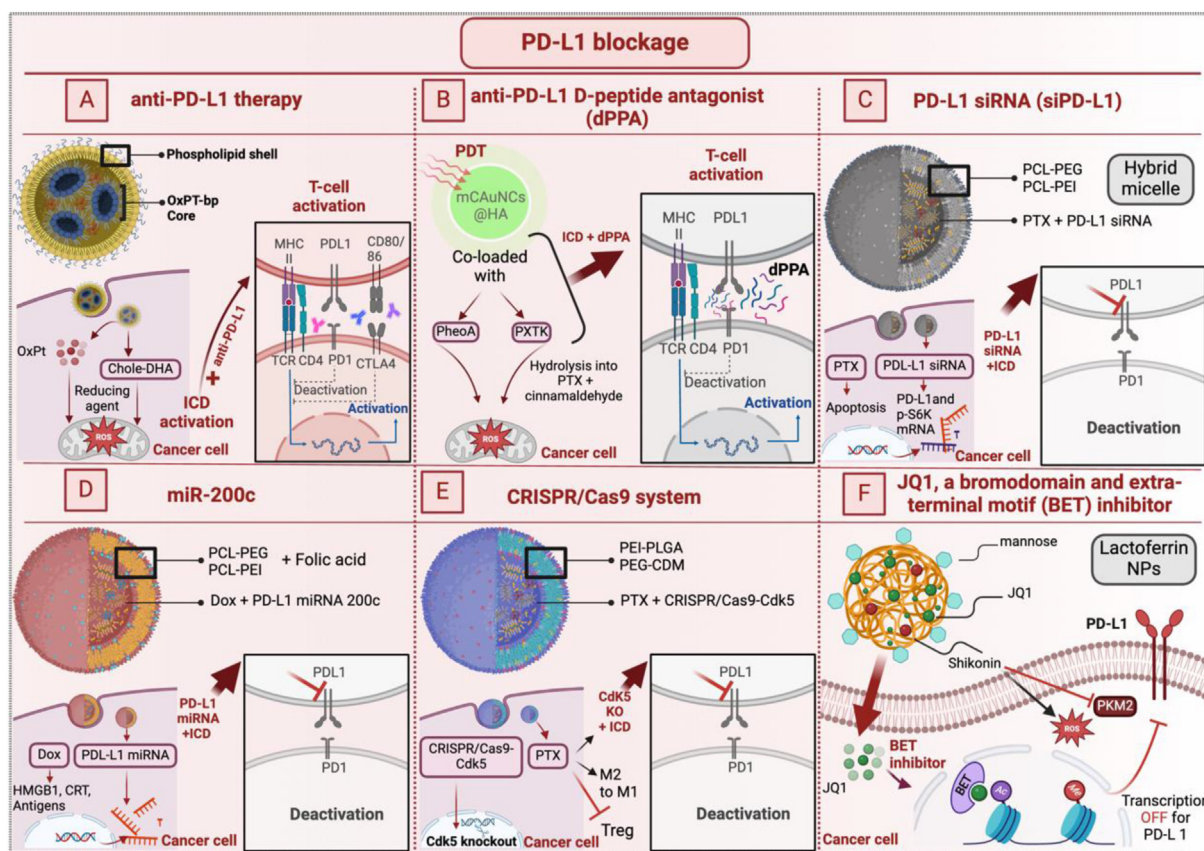


Figure 4 PD-L1 blockade synergistically enhances the antitumor immunity elicited by ICD inducer nanomedicines. (A) anti-PD-L1 therapy plus OXA/DHA enhanced ROS generation showing increased tumor infiltration of DCs and macrophages thus enabling powerful antigen uptake and presentation, and increased density of CD8⁺ T cells in tumors⁸. (B) Anti-PD-L1 D-peptide antagonist combined with PTX/pheophorbide NPs alleviated the immunosuppressive TME and enhanced the function of CTLs⁹⁴. (C) *siPD-L1* and PTX PEGylated PCL/PEI hybrid micelles enhanced the anti-tumor immune response⁹⁵. (D) Combined delivery of *miR-200c* and DOX via PLGA-PEI NPs safeguarded *miR-200c* from degradation, and enhanced the sensitivity of cancer cells to DOX⁹⁶. (E) Co-delivery of CRISPR/Cas9-Cdk5 plasmid (Cas9-Cdk5) and PTX via PEGylated PEI-PLGA NPs successfully silenced the PD-L1 and interfered with IFN- γ signaling⁹⁷, and (F) JQ1 co-loaded with SHK into mannose-modified lactoferrin NPs decreased PD-L1 expression and reduced the tumoral infiltration of Tregs²⁷ (created via BioRender).

of the released drugs was exploited to induce ICD and hence potentiate the efficacy of anti-PD-L1 therapy. Two days following treatment of MC38 tumor-bearing mice with OXA/DHA NPs and α PD-L1, there was an increase in tumor infiltrating CD11c⁺ DCs, F4/80⁺ macrophages and CD8⁺ T cells in tumors, thereby amplifying the potency of checkpoint blockade immunotherapy. Consequently, the development of new tumors was hindered for the subsequent month in contrast to 100% tumor formation observed in untreated mice⁸. Similar synergized anti-tumor immune responses and cancer cell killing were obtained when DOX-loaded PEGylated PLGA NPs were combined with anti-PD-1 antibodies in murine B16F10 melanoma model⁹³.

Even though the FDA has approved numerous monoclonal antibodies targeting PD-1/PD-L1 pathway for use in clinical treatments, those macromolecular antibodies suffer from low response rate, poor tumor penetration, poor stability, immunotoxicity, and high manufacturing costs which impede their translation. Therefore, a hydrolysis-resistant anti-PD-L1 D-peptide antagonist (dPPA) showed higher stability while blocking the PD-1/PD-L1 pathway. dPPA was adsorbed *via* electrostatic interaction onto PTX/pheophorbide co-loaded NPs to relieve the immunosuppressive TME and improve the activity of CTLs triggered by PDT-mediated ICD⁹⁴. In 4T1 tumor bearing mice, single PDT NPs or PD-L1 blockade alone inhibited 65.4% of tumor growth. However, a combined dPPA with the NPs increased the growth inhibition rate to 84.2% (Fig. 4B).

Similarly, anti-PD-L1 peptide (CVRARTR) was coupled to DOX *via* a cathepsin B-specific cleavable peptide (FRRG) to form self-assembled NPs. The NPs were internalized into 4T1 cancer cells *via* PD-L1 receptor-mediated endocytosis⁹⁸. The cancer cell upregulated cathepsin B resulted in release of DOX which induced powerful ICD, with enhanced CRT translocation and release of HMGB1. Meanwhile, the immune inhibitory PD-1/PD-L1 binding was interrupted *via* lysosomal PD-L1 degradation due to potent binding affinity to PD-L1.

RNA interference approaches offer a different strategy for reducing PD-L1 expression. Compared to monoclonal PD-L1 antibodies that can induce autoimmune side effects by binding to normal tissues, *PD-L1 siRNA (siPD-L1)* is highly selective to tumor cells and induces long-term PD-1/PD-L1 blockade by inhibiting *de novo* synthesis of PD-L1. Nanocarriers were successfully designed to overcome delivery challenges of siPD-L1 by protecting it against degradation by nucleases and facilitating endosomal escape for efficient cytosolic delivery⁹⁵. Co-encapsulation of siPD-L1 with PTX into PEGylated PCL/PEI hybrid micelles has enhanced the PTX-induced anti-tumor immune response by decreasing the expression of PD-L1 and hence blocking PD-1/PD-L1 binding and thus inhibited the tumor growth of B16F10 melanoma bearing mice (Fig. 4C)⁹⁵.

Another approach utilizes delivery of microRNA to inhibit PD-L1 expression. The reduced level of *miR-200c*, a member of microRNA-200 family, resulted in overexpression of PD-L1 in cancer cells which causes exhaustion of T cells. Accordingly, tumor-targeted delivery of miR-200c together with DOX *via* PEGylated PLGA-PEI NPs prevented serum degradation of miR-200c and effectively inhibited the PD-L1 expression⁹⁶. As a result, the NPs increased the response of NCI-H1299 and MC38 cells to ICD mediated immune response elicited by DOX leading to enhanced maturation of DCs and increased infiltration of CD8⁺ T cells (Fig. 4D).

Traditional siRNA therapy can only interfere with the process of gene translation and impairs the expression of oncogenic

proteins. However, the original copy of the oncogenes remains intact. In contrast, *CRISPR/Cas9 system* can effectively target and excise target genes with the guide of sgRNA and Cas9 endonuclease activity. Therefore, to attenuate PD-L1 expression permanently, pH-responsive PEGylated PEI-PLGA NPs successfully co-delivered CRISPR/Cas9-Cdk5 plasmid (Cas9-Cdk5) and PTX⁹⁷. In this manner, expression of IFN γ was targeted by knocking-out cyclin-dependent kinase 5 (Cdk5) gene (Fig. 4E). This led to PD-L1 downregulation by tumor cells and restored the CTL-mediated antitumor immunity. In addition, the NPs triggered ICD resulting in maturation of DCs, reduced infiltration of Tregs, and improved M2/M1-polarization of TAMs in the TME, thus inhibiting growth and prolonging survival of B16F10-bearing mice⁹⁷.

In another strategy, PD-L1 expression in cancer cells was also reduced by using *JQ1*, a bromodomain and extra-terminal motif (BET) inhibitor. It was reported that SHK/JQ1-loaded mannose-modified lactoferrin NPs bind successfully to LRP1 and mannose receptors, respectively overexpressed by cancer cells and M2 macrophages²⁷. After internalization into CT26 colon cancer cells and M2 macrophages, SHK efficiently induced ICD and polarization of TAMs from immunosuppressive M2 to antitumoral M1 phenotype while JQ1 promoted downregulation of PD-L1 and reduced infiltration of Tregs (Fig. 4F).

4.1.2. CTLA4 blockade

CTLA-4 is an inhibitory receptor expressed predominantly on T cells and competes with CD28, a costimulatory molecule on T cells, for binding to B7 molecules (CD80 and CD86) on APCs, leading to dampening T cell activation⁹⁹. Antibodies targeting CTLA-4 such as ipilimumab block this interaction, thereby preventing the inhibitory signaling allowing for more robust and prolonged T cell activation. Liposomal DOX (Doxil) exhibited enhanced antitumor immune response when combined with CTLA-4 mAbs resulting in synergistic antitumor efficacy and increased survival rate in CT26 mouse tumor model¹⁰⁰. The combined PDT and magnetic hyperthermia mediated by Ce6-Fe₃O₄ NPs@disulfide-bridged MSNs triggered ICD, resulting in CRT exposure and HMGB1 release which boosted the anti-metastatic effect of anti-CTLA-4 antibody⁹². This was reflected as enhanced release of TNF- α , IFN- γ , and IL-6, leading to improved DC maturation, increased CTL infiltration, and Treg inhibition in MCF-7 and 4T1 tumors.

4.1.3. TNFR agonists

The TNFR superfamily consists of various receptors, including TNFR1, TNFR2, OX40, and 4-1BB, among others. These receptors are expressed on various immune cells, including T cells, B cells, DCs, and NK cells¹⁰¹. Binding of ligands to TNFR can activate multiple signaling pathways, crucial for immune cell activation and survival. Therefore, TNFR agonists targeting OX40, 4-1BB, or CD27 are used to promote T cell activation and enhance the immune response against cancer. By inducing ICD, liposomal DOX (Doxil) showed synergistic activity with TNFR OX40 and glucocorticoid-induced TNFR-related (GITR) ligand fusion proteins thus enhancing their immunostimulatory effects in either CT26 or MCA205 tumor models¹⁰⁰. Both DOX and TNFR agonists provoked powerful immune response as demonstrated by enhanced maturation of DCs, depletion of Tregs and increased infiltration of CD8 cytotoxic T cells.

4.2. Immunoadjuvants

4.2.1. Toll-like receptor (TLR) agonists

CpG oligonucleotides are single-stranded sequences of nucleotides that include unmethylated cytosine–phosphate–guanine motifs that bind to TLR-9. Although local administration of CpG-oligonucleotides can induce a systemic antitumor immune response as an immunoadjuvant, rapid leakage of free CpG from injection site usually results in untoward toxicity¹⁰². Therefore, DOX and genipin-crosslinked CpG PEI NPs were combined into an injectable cyclodextrin-PEG hydrogel for prolonged immunostimulatory effect. The ICD induction by DOX together with the immunostimulatory effect of CpG promoted DC maturation resulting in increased infiltrating CTLs, and reduced proportion of MDSCs and M2-TAMs (Fig. 5A)¹⁰².

The immunoadjuvant monophosphoryl lipid A (MPLA), a TLR-4 agonist, is reported to enhance and prolong the immune response when combined with vaccine antigens. Therefore, MPLA was combined with DOX as ICD inducer *via* DSPE-PEG micelles to enhance its antitumor immune response¹⁰⁵. DOX micelles induced sufficient release of TAAs that elicited powerful immune

response however not completely inhibited tumor growth. Combination with MPLA enhanced the DC maturation and promoted the macrophage phagocytic capability. However, MPLA stimulated T cells to produce IFN- γ which increases PD-L1 expression resulting in immunosuppression. Therefore, anti-PD-L1 antibodies were co-administered with the micellar combination resulting in completely eradicated B16F10 tumors in mice¹⁰⁵. Likewise, hydrophobic Ce6 and MPLA were jointly encapsulated in the core of self-assembled NPs made from an amphiphilic phenylalanine derivative of poly(glutamic acid)¹⁰⁶. Forty days post-inoculation of the primary tumor into mice, those treated with the NPs exhibited 100% survival. Imidazoquinolines (IMDQs) were combined with DOX into pH/redox-responsive self-assembled NPs¹⁰⁷. The NPs sequentially responded to the acidic TME at tumor sites (pH 6.5–6.8) and endosome compartments (around pH6.0) of DCs at lymph nodes to deliver DOX and IMDQs to target cancer and immune cells, respectively. DOX induced ICD while IMDQ specifically stimulated TLR-7/8 to enhance DC maturation and antigen presentation¹⁰⁷. The NPs elicited a potent anti-tumor immunity against both primary and distant (abscopal) B16-OVA and CT26 tumor mouse models. As mentioned earlier,

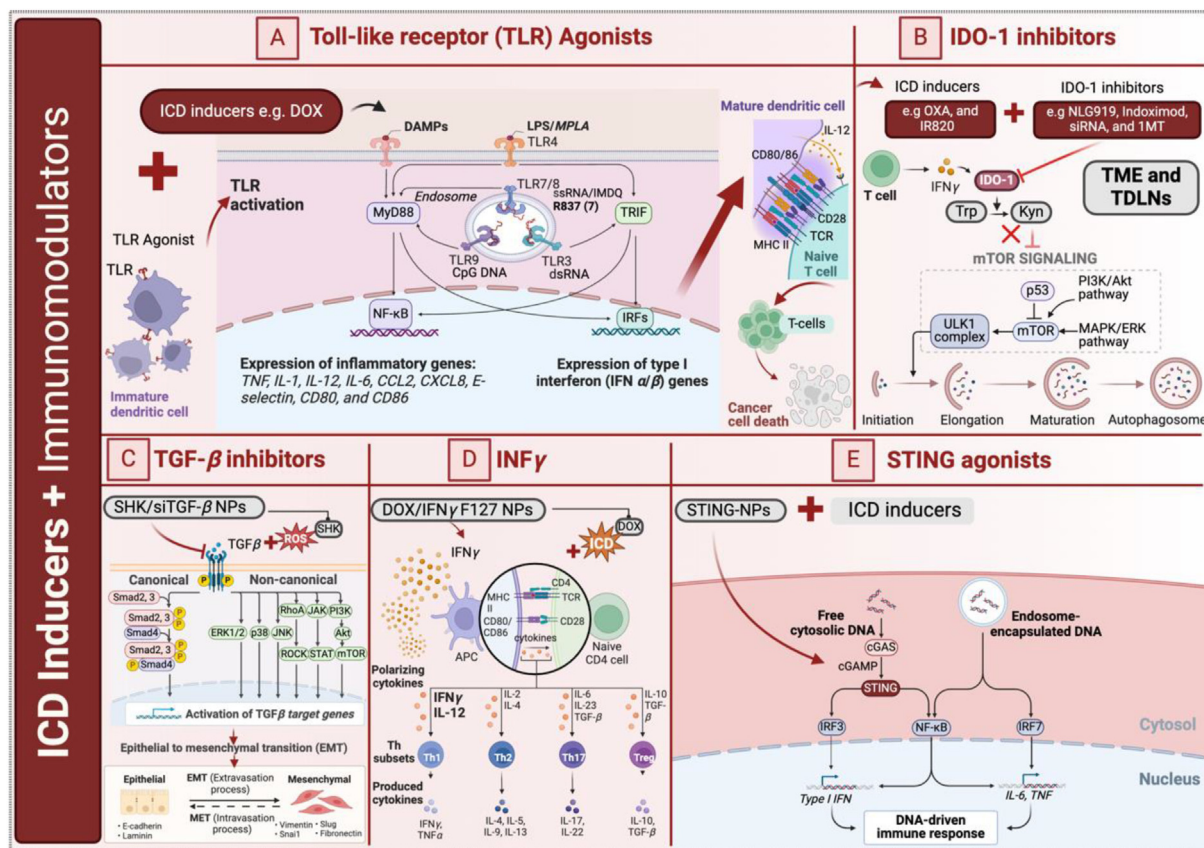


Figure 5 Immunoadjuvants synergistically boost the antitumor immune response triggered by ICD inducer nanomedicines. (A) TLR agonists such as MPLA, CpG and imiquimod enhance DC maturation, and antigen presentation and hence increase T cell infiltration to promote ICD response. (B) Indoleamine 2,3-dioxygenase 1 (IDO-1) inhibitors, such as NLG919, indoximod, and 1-MT were used to overcome immunosuppression by preventing degrading tryptophan (Trp) and accumulating kynurenine (Kyn) in TME. Kyn suppresses the activity of CD8⁺ T cells, activates Tregs and inhibits the mTOR pathway and hence autophagy²³. (C) TGF- β inhibitors such as TGF- β siRNA was combined with SHK as ICD inducer *via* PEI NPs, where efficient TGF- β silencing reversed the TGF- β -based immunosuppression and increased infiltration of CTLs¹⁰³. (D) INF γ , combined with DOX-PLGA NPs, promoted DC maturation, and increased the level of IL2 and TNF and enhanced tumor infiltration of CTLs³⁴, and (E) STING agonists, loaded into PEGylated poly(methacrylate) NPs stimulated cGAS/STING pathway resulting in enhanced ICD of neuroblastoma cells and activated interferon-stimulated genes¹⁰⁴ (created *via* BioRender).

Imiquimod (R837) PLGA NPs, a TLR-7 agonist, synergistically enhanced the ICD inducing antitumor immune response when combined with X-ray radiotherapy²⁸.

4.2.2. IDO-1 inhibitors

The immunosuppressive TME can reduce the efficacy of ICD triggered by some chemotherapeutics. The secreted IFN- γ by CTLs activates the immune response by different mechanisms. However, it also increases the activity of IDO-1 which is up-regulated in tumor-draining lymph nodes (TDLNs) and tumor tissues. IDO-1 provokes immunosuppression by degrading tryptophan and accumulating kynurenine in TME leading to suppressed activity of CD8⁺ T cells and activating Tregs. Moreover, tryptophan depletion by IDO induces immunosuppression in the TME by suppressed mTOR pathway and hence autophagy inhibition¹⁰⁸. Hence, the inhibition of IDO1 leads to stimulation of the mTOR1 signaling and activates autophagy, which is critical for ATP release during ICD (Fig. 5B). In addition, the increased degradation of tryptophan also affects the activity of DCs in TDLNs by reducing the activity and numbers of APCs which in turn decreases the numbers of infiltrating antigen-specific T cells¹⁰⁹. Therefore, IDO-1 inhibitors were combined with ICD inducers *via* nanomedicines.

A disulfide bond-crosslinked homodimer of the IDO-1 inhibitor, NLG919 was self-assembled with PEGylated OXA prodrug to form charge-reversible NPs²³. In TME acidity, the PEG shell was removed exposing the NPs to reverse their charge from negative to positive to increase internalization and penetration within tumor tissue. While OXA elicited antitumor immune response and increased tumoral infiltration of CD8⁺ T cells, NLG919 inhibited IDO-1 mediated immunosuppression by suppressing the activity of Tregs. The NPs effectively inhibited the growth of breast and colorectal primary tumor and metastasis models²³. Similar combinations of OXA with IDO inhibitor, indoximod¹¹⁰ or IDO1 siRNA¹¹¹ were also reported to synergistically enhance the antitumor immune response *via* phospholipid bilayer-coated mesoporous silica NPs and cationic lipid-assisted PEG-*b*-PLGA NPs, respectively^{110,111}. Similarly, IDO inhibitor 1 MT was conjugated with the organic PTT agent IR820 to self-assemble into NPs¹¹². The laser-activated IR820-1 MT NPs significantly boosted the infiltration of cytotoxic T cells, helper T cells, and memory T cells while reducing the proportion of Treg cells. This led to highly effective immune response to tumor metastasis. A similar combination of ICD inducer MTX and IDO1 siRNA was enabled *via* size-reducible dimethylmaleic anhydride-grafted PEGylated poly(L-lysine) copolymer NPs showing high tumor penetration and efficient immune response in 4T1 and CT26 bilateral tumor models¹¹³.

4.2.3. TGF- β inhibitors

The overexpression of TGF- β , a main immunosuppressive marker in TME, enhances deposition of the dense collagen-rich tumor extracellular matrix (ECM) that hinders immune cell infiltration including effector T cells and promotes the proliferation of Tregs and inhibits the expansion of APCs. Therefore, TGF- β siRNA (siTGF- β) was combined with SHK as ICD inducer *via* PEI NPs (Fig. 5C)¹⁰³. While FA surface modification enhanced their uptake into 4T1 cancer cells, the PEI facilitated lysosomal escape of siTGF- β *via* its proton sponge effect. Successful inhibition of TGF- β reduced the immunosuppression resulting in increased infiltrating CTLs, reduced proliferation of Treg cells and restricted

lung metastasis¹⁰³. Thus, SHK/siTGF- β NPs demonstrated 88.5% delayed tumor growth and prevented lung metastasis.

4.2.4. Interferon gamma (IFN γ)

DOX was conjugated *via* pH-sensitive hydrazone bond to the PLGA core of thermosensitive NPs whereas IFN γ was electrostatically and thermodynamically absorbed into the pluronic F127 shell (Fig. 5D)³⁴. The NPs exhibited synergistic antitumor immune response in B16F10 tumor bearing mice. As a potent immunomodulatory, IFN γ enhanced maturation of DCs, and triggered immune response against melanoma as reflected as increase in the level of IL-2 and TNF and reduced levels of immunosuppressive cytokines, including IL-10 and TGF β and hence increased infiltration of CTLs³⁴.

4.2.5. STING agonists

Cyclic dinucleotide (CDN) agonists of the stimulator of interferon genes (STING) pathway have been considered among the efficient tools to increase the immunogenicity of cancer cells *via* stimulating innate immunity. STING agonists can activate DCs through IFN-I and enhances their cross-presentation of tumor antigens for priming of CD8⁺ T cells and hence increases their tumor infiltration¹⁰⁴. Moreover, stimulation of cGAS/STING pathway was reported to provoke ICD in some cancer cells and hence activating antitumor T cell immunity. However, CDNs suffer efficient delivery to the cytosol due to their highly water-soluble negatively charged structure and rapid intracellular degradation. Therefore, STING activating PEGylated poly(methacrylate) NPs enabled endosomal escape and delivery of the STING agonist 2'3'-cGAMP to the cytosol of neuroblastoma cells to activate IFN-stimulated genes including increased phosphorylation of interferon regulatory factor 3 (IRF3) compared to free cGAMP (Fig. 5E)¹⁰⁴. In a model of neuroblastoma, the STING-NPs enhanced extracellular secretion of ATP and HMGB1 and surface exposure of CRT by NB cells leading to be efficiently phagocytosed by DCs. *In situ* vaccination with STING-NPs protected most of the mice from tumor recurrence after their inoculation with live Neuro-2a cells¹⁰⁴. Combining anti-PD-L1 antibodies with STING-NPs synergistically showed higher anti-tumor efficacy compared to single anti-PD-L1 therapy.

In addition to their role in provoking anti-tumor immunity by their own ICD inducing mechanisms, STING agonist could be used to induce a condition of synthetic immunogenic cell death (sICD) where the cGAMP acts as an exogenous immunogenic adjuvant to cancer cells followed by treatment with cytotoxic chemotherapy. This approach simulates the consequent events in natural ICD and generates STING-agonist loaded immunogenic cellular debris that provides simultaneous exposure of APCs to both tumor antigens and cGAMP. STING agonist-loaded PLGA nanoshells achieved about 41% efficient entrapment of the water-soluble cGAMP¹¹⁴. The cGAMP-loaded NPs were incubated with cancer cells (CT26, B16F10, or HeLa cells) for 24 h prior to treatment with cytotoxic drugs including non-ICD inducers (*e.g.*, cisplatin) and ICD inducers (*e.g.*, DOX). The use of NPs resulted in the production of cGAMP-loaded cellular debris which concurrently transfer the tumor antigens to DCs to stimulate type-I IFN signaling. Therefore, co-culture of the generated cellular debris with murine DCs for 48 h caused maturation of DCs as shown by up-regulation of CD80 and CD86 in comparison to free cGAMP-treated and non-adjuvanted debris¹¹⁴. In mouse models of CT26 colon cancer and B16F1 melanoma, cGAMP NPs were intratumorally injected to initiate sICD, followed by irinotecan or

cisplatin, resulting in powerful tumor regression together with remarkable increased antigen-specific T cell response.

In another investigation, cationic silica NPs (CSiNPs) were electrostatically complexed with the anionic STING agonist cGAMP²¹. The positively charged CSiNPs strongly bind with cancer cells resulting in disruption of their plasma membrane in addition to ROS generation that induce oxidative stress resulting in necrotic cell death with the release of TAAs. After their intratumoral administration into B16F10 murine melanoma model, the CSiNPs/cGAMP nanocomplex resulted in powerful stimulation of DCs as revealed by increased CD80+ MHCII + cells in TME, and strong tumor suppression together with the development of adaptive memory showing resistance to secondary tumor cell challenge²¹. Therefore, activating cGAS–STING pathway in cancer cells can either induce ICD or act as immune adjuvant to help cytotoxic chemotherapeutics to induce ICD resulting in enhanced adaptive T cell anti-tumor immunity.

4.3. Anti-cancer vaccines

A therapeutic vaccine can be combined with ICD inducer nanomedicine to boost the antitumor immune response. Therefore, the ICD inducing MTX-loaded PEGylated PLGA NPs were co-administered with an anti-cancer DNA vaccine composed of plasmid encoding an epitope derived from glioblastoma-associated antigen (pTOP) into GBM-bearing mice¹¹⁵. The vaccine enhanced the immunogenic response by stimulating antigen release and presentation in the brain. As a result, the combined approach increased the M1/M2 macrophage ratio and IFN- γ -secreting CD4⁺ and CD8⁺ T cells thus prolonged the survival of GL261-bearing mice.

4.4. Stromal modulators

Cancer associated fibroblasts (CAFs), the most abundant stromal cells, generate immunosuppressive TME which in turn reduces the efficacy of ICD inducers. Trypsin secreted by mast cells was found to induce differentiation of stromal fibroblasts into CAFs via protease-activated receptor-2 (PAR-2) signal pathway¹¹⁶. Therefore, CAF reprogramming trypsin inhibitory NPs were combined with liposomal DOX to enhance its ICD inducing potential¹¹⁷. The molecularly imprinted NPs synthesized using mesoporous silica as a carrier and trypsin as a template molecule could bind to trypsin with high affinity and selectivity and inhibited its activity. As a result, the NPs reversed the activated phenotype of CAFs as denoted by α SMA downregulation in NIH-3T3 fibroblasts, relieved the stromal barrier and enhanced the tumor penetration of DOX liposomes. Consequently, the ICD inducing efficacy of DOX in 4T1 tumor bearing mice was enhanced along with increased infiltration of CD4⁺, CD8⁺ T cells and NK cells.

4.5. Phagocytosis enhancers

Anti-CD47 monoclonal antibodies were co-administered with a lipid nanomedicine to simultaneously enhance ICD and phagocytosis of cancer cells. OXA and the PS pheophorbide A were coupled to PEGylated lipid vesicles via acid sensitive 2,3-dimethylmaleic anhydride and peptide linkers, respectively¹¹⁸. In the acidic pH and upregulated MMP-2 of the TME, the PEG layer was cleaved and the released OXA and PS induced ICD of

4T1 cancer cells with laser irradiation and markedly enhanced CRT expression. However, tumor cells overexpress CD47 “don’t eat me signal” that binds with Sirp α on macrophage surface to prevent phagocytosis of cancer cells and this counteracts the “eat me” effect of CRT. Therefore, combination of the ICD triggering NPs with CD47 blockade enhanced the antigen presenting and phagocytic capacity of DCs. CD47 antibodies alone inhibited less than 30% of the primary tumor growth. However, combination of NPs with CD47 blockade exerted the highest antitumor efficiency by completely suppressing growth of the distant tumors¹¹⁸. Similarly, combining DOX and CD47 blockage was enabled via 20 nm FHSirp α nanocages formed by self-assembly of human ferritin engineered to contain a Sirp α variant¹¹⁹. The nanocage binds and blocks CD47–Sirp α pathway resulting in 1.9–11.2-fold enhanced phagocytosis of HT29 colon cancer cells by macrophages compared with untreated controls¹¹⁹.

CD24 sialic-acid-binding Ig-like lectin 10 (Siglec-10) pathway was recently identified as another phagocytosis inhibitory checkpoint. Antibodies against CD24, “don’t eat me signal” overexpressed by cancer cells, were coupled to the surface of PCL-PEI NPs loaded with celastrol. aCD24 blocked the binding of tumoral cell CD24 with SIGLEC10 on macrophages resulting in enhanced phagocytosis of cancer cells^{120,121}. Meanwhile, celastrol provoked ICD of 4T1 breast cancer cells with increased expression of CRT. As a result, the percentage of CD80⁺CD86⁺ matured DCs in lymph nodes and tumor infiltrating CD8⁺ CTLs have been increased whereas the frequency of Tregs and MDSCs was significantly reduced.

4.6. Macrophage polarizers

Bacterial therapy is reported to activate the body’s immunity and therefore it can suppress tumor growth and metastasis. Moreover, bacteria could induce different patterns of macrophage polarization. The characteristic tumor hypoxia can further help growth and colonization of anaerobic bacteria within the hypoxic necrosis zone of the tumor. Because of their tumor targeting ability, bacteria were successfully used to deliver therapeutic agents to a tumor. Therefore, the TLR7/8 agonist resiquimod (R848)-loaded PLGA NPs were electrostatically anchored onto the surface of glycol chitosan-decorated non-pathogenic bacterium *Escherichia coli* MG1655 (Ec-PR848)¹²². The Ec-PR848 were efficiently accumulated within the hypoxic tumor and once phagocytosed by M2 macrophages, the released R848 along with *E. coli* polarized M2-TAMs into M1-TAMs. In parallel, DOX-loaded PLGA NPs were co-administered to induce ICD which further activated the antitumor immunity resulting in tumor elimination¹²².

Another interesting approach utilizes modulating mitochondrial dynamics to induce macrophage polarization. Given that Mitofusin 1 (MFN1) is essential for preserving mitochondrial morphology, M2-TAM targeted NPs loaded with a specific short hairpin RNA (shMFN1) effectively suppressed MFN1 and prevented mitochondrial fusion in TAMs, thereby encouraging mitochondrial fission and shifting the phenotype of M2-TAMs to M1-TAMs^{123,124}. In parallel, cancer cells were targeted using charge-reversible DOX NPs to induce ICD. The anionic PEG-DMMA shell of the NPs facilitated extended circulation. This shell was then detached from the NP surface in response to the tumor acidic pH, causing a reduction in size and a shift to a positively charged surface resulting in promoted penetration and internalization within cells. The ICD of cancer cells induced by DOX-NPs, in combination with repolarization of M2-TAMs

instigated by shMFN1-NPs, collaboratively reversed the immunosuppressive TME¹²⁴. Therefore, the combination of both NPs displayed strong tumor growth suppression in 4T1 subcutaneous tumor-bearing mice.

When combined with MPLA, a Toll-like receptor 4 (TLR4) agonist, hydroxyapatite NPs (HANPs) synergistically enhanced polarization of RAW264.7 macrophages to M1 antitumoral phenotype. As a result, the NPs increased secretion of stimulatory cytokines TNF α and IL-6¹²⁵. Moreover, HANPs induced ICD of 4T1 cells revealed by increased expression of HMGB1, CRT and ATP. HANPs and MPLA synergistically suppressed 4T1 tumor growth in a mouse model. HANPs are anticipated to stimulate ICD by acting like calcium electroporation after the burst of cancer cells resulting in elevated intracellular Ca²⁺. Therefore, HANPs upregulated the expression of HMGB1 and the production of inflammatory cytokines by promoting the intracellular influx of calcium.

4.7. Hypoxia modulators

Tumor hypoxia, a characteristic of TME, is primarily produced by the increased oxygen consumption after ATP generation during mitochondrial oxidative phosphorylation^{126,127}. Moreover, among various ICD inducers, PDT requires oxygen to generate ROS *via* photochemical reactions, however; the oxygen deficiency due to the tumor hypoxia remarkably limits the PDT efficacy of ICD

induction. In the other direction, the excessive oxygen consumption during PDT exacerbates the tumor hypoxia¹²⁸. Tumor hypoxia significantly contributes to drug resistance and immunosuppression. Hypoxia elevates the ROS level resulting in upregulation of hypoxia-inducible factor (HIF-1 α) and vascular endothelial growth factor (VEGF) involved in tumor angiogenesis and progression. Moreover, hypoxia promotes metabolic acidosis in cancer cells which also contributes to development of drug resistance and suppression of intratumoral infiltration and activity of CTLs in addition to upregulation of MDSCs and recruiting Tregs thus resulting in immunosuppressive TME which markedly impairs the ICD-mediated antitumor immune response¹²⁹. To overcome this challenge, novel modalities to overcome tumor hypoxia should be combined with ICD-inducing nanomedicine.

4.7.1. Hemoglobin

The use of ER-targeted indocyanine green (ICG) coupled with gold nanospheres to induce PDT under laser irradiation of CT26 cells resulted in excessive oxygen consumption and hypoxia. Therefore, by virtue of the oxygen carrier ability of hemoglobin, hemoglobin-loaded liposomes were used as an adjuvant to release oxygen to the hypoxic TME and thus compensate the ROS consumption by PDT and enhance the PDT-induced ER-stress (Fig. 6A)¹³⁰. After combination with hemoglobin-liposomes, the generation of ¹O₂ was increased and hence the cytotoxicity of NPs

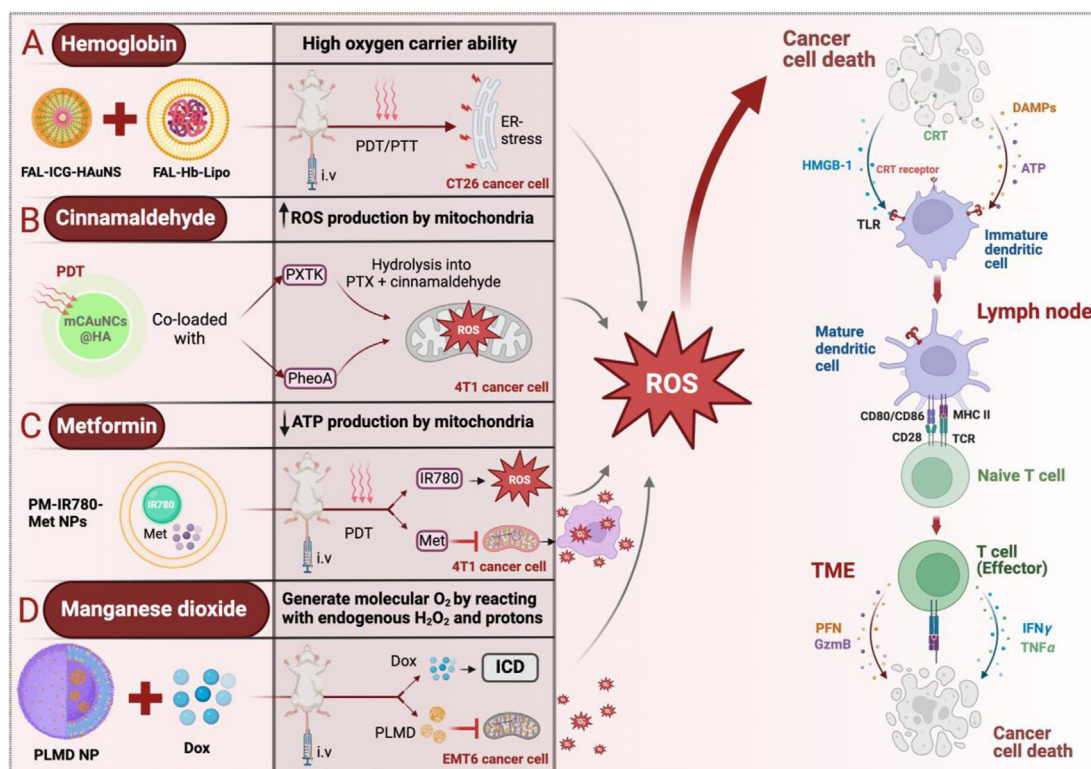


Figure 6 Hypoxia modulators overcome tumor hypoxia and synergistically promote ICD inducer nanomedicine-mediated immune response. (A) Hemoglobin-loaded liposomes enhanced oxygen release to the hypoxic TME and hence potentiated the PDT-induced ICD by ICG-coupled gold nanospheres¹³⁰. (B) Cinnamaldehyde was co-loaded with PTX dimeric prodrug into PheoA-gold nanoclusters to enhance ROS generation by mitochondria to overcome PDT-induced hypoxia⁹⁴. (C) Metformin was incorporated into IR780-loaded NPs to reduce ATP production by mitochondria and improve tumor oxygenation thus potentiates PDT-mediated ICD immunity¹²⁹, and (D) manganese dioxide (MnO₂) NPs were combined with DOX to generate molecular oxygen (O₂) and reversed the tumor hypoxia and therefore potentiated DOX-triggered ICD induction¹³¹ (created *via* BioRender).

to CT26 cells has been increased from 20% to about 46% under hypoxia¹³⁰.

4.7.2. Cinnamaldehyde

A PTX dimeric prodrug was chemically coupled to the PS PheoA-encapsulated hyaluronate gold nanoclusters using ROS-responsive cinnamaldehyde and thioacetal linker (Fig. 6B)⁹⁴. At the higher ROS concentration in tumor cells, the resultant hydrolytic product cinnamaldehyde increased ROS production by mitochondria to compensate its irreversible consumption by thioacetal cleavage and hence increased the PheoA-mediated PDT efficacy⁹⁴. As a result, the infiltration of CD4⁺, CD8⁺ T cells and NK cells has been increased with enhanced release of TNF- α and IL-12 and 84.2% tumor growth suppression. Self-cycling DTX-loaded NPs were developed to continuously self-supply ROS to enhance ICD response of DTX. Cinnamaldehyde as ROS-generating agent and 4-hydroxymethylphenylboronic acid pinacol ester (HPAP) as a ROS-responsive moiety were coupled to DTX-loaded cyclodextrin¹³². First, the endogenously generated ROS facilitated degradation of HPAP resulting in release of DTX to induce ICD of 4T1 cells. The degradation products of HPAP then created acidic microenvironment leading to acetal cleavage to release cinnamaldehyde. The released cinnamaldehyde in turn induces the generation of more ROS through mitochondrial damage, resulting in amplified DTX release. The NPs suppressed the growth of 4T1 tumors in a mouse model and inhibited lung metastasis.

4.7.3. Metformin

Metformin, as an inhibitor of oxidative phosphorylation, was incorporated into the PS IR780-loaded NPs to enhance their PDT-mediated ICD immune response. Metformin interferes with mitochondrial respiration to prevent ATP production and hence inhibits the oxygen consumption by tumor¹²⁹. After accumulation into tumor, the PDT, mediated by IR780, successfully eliminated 4T1 cancer cells by generating ROS while metformin improved tumor oxygenation (Fig. 6C). Consequently, the reversed tumor hypoxia enhanced the PDT-triggered ICD of cancer cells and impeded MDSC-regulated immunosuppression and increased T cell recruitment thereby helps eliminate the primary tumors and inhibit tumor metastasis¹²⁹.

4.7.4. Manganese dioxide (MnO₂) NPs

MnO₂ NPs reacts with endogenous H₂O₂ and protons (mild acidic medium of tumor) to generate molecular oxygen (O₂). Combining MnO₂ with DOX successfully reversed the tumor hypoxia and hence reduced the intratumoral expression of HIF-1 α and VEGF as well as the drug resistance proteins P-gp, carbonic anhydrase IX, and mutated p53 and also induced TAM polarization to M1 phenotype (Fig. 6D)¹³¹. Thus, the NPs enhanced DOX-induced ICD and cytotoxicity and increased tumor-infiltrated CD8⁺ T cells¹³¹. Therefore, i.v. injection of DOX/MnO₂ NPs achieved 60% tumor regression and increased survival time in orthotopic murine EMT6 breast tumor. Similarly, hyaluronic acid and MnO₂ NPs were used to coat gold nanocage (AuNC) for enhancing their selective delivery to colorectal cancers and improving tumor oxygenation that boosts the ICD response mediated by AuNC core NIR-triggered PDT, respectively¹³³. *In vivo*, the NPs succeeded in tumor targeting and produced sufficient oxygen to alleviate tumor hypoxia and consequently inhibited the tumor growth and recurrence.

In a similar context, polymer-lipid MnO₂ NPs were developed to boost the antitumor immune response of radioresistant tumors

by overcoming hypoxia¹³⁴. The NPs increased the local oxygen levels of castration-resistant prostate tumor thus enhanced the sensitivity of the hypoxic tumor to radiation-mediated ICD. Compared to radiation alone, pre-treatment of murine TRAMP-C2 prostate cancer cells with those NPs enhanced the DNA double strand breaks due to promoted autophagy and ER stress. In a syngeneic TRAMP-C2 tumor model, the NPs improved radiation-induced ICD with increased release of DAMPs, infiltration of CD8⁺ T cells and polarization of RAW264.7 macrophages to M1 phenotype resulting in suppressed tumor growth.

4.8. Autophagy modulators

Autophagy is an innate homeostatic mechanistic pathway that mediates the degradation of cellular senescent organelles and proteins. Autophagy acts as “enabler” that can boost ICD by enhancing ATP secretion from the lysosome of cancer cells which can stimulate purinergic receptors and therefore promote anti-tumor immunity. Mitophagy, the mitochondrial selective autophagy, is necessary for production of ATP and therefore autophagy activators can enhance the antitumor immunogenic response triggered by ICD inducers¹³⁵. Thus, the immunomodulatory drug icaritin triggered both mitophagy and apoptosis in mouse Hepa1-6 and human Huh7 hepatocellular carcinoma cells, thereby inducing ICD. Therefore, PEGylated PLGA NPs co-loaded with icaritin and DOX synergistically induced ICD and remodeled the immunosuppressive TME and hence efficiently improved anti-HCC effect in mouse HCC model¹³⁵. On the other hand, autophagy plays dual roles in ICD progression. DAMPs and antigens such as MHC-I, which activate innate immunity, were known to be captured and degraded by autophagosomes. Thus, activating autophagy in the TME can engulf immune-related antigens, thus suppressing the adaptive immune response, leading to tumor evasion. Therefore, autophagy inhibitor (hydroxychloroquine, HCQ) was co-loaded into liposomes with SHK to boost its induced ICD and enhance antigen exposure in colon cancer immunotherapy¹³⁶. ATP was added as an inner phase for remote loading gradient of the liposomes to compensate the ATP loss due to autophagy inhibition. After treatment with liposomes, several antigens were exposed on the membrane of the CT26 colorectal cancer cells due to inhibited autophagy¹³⁶. Systematic determination of moderate doses of combined liposomes resulted in the most powerful immune response and inhibited tumor growth. Thus, inhibiting autophagy at an optimal dose improved the surface antigenicity elicited by ICD inducers.

4.9. Miscellaneous synergistic agents

4.9.1. Wnt5a/ β -catenin blockade

In BRAF-mutant melanoma cells, the overexpressed protein Wnt family member 5A (Wnt5a) is involved in tumor immune evasion and immunotherapy resistance. Mechanistically, Wnt5a mediates immunosuppression and promotes tumor growth and metastasis by inducing localized DC tolerance and hence reduces the antigen presenting capacity of DCs and preventing T cell infiltration as well as inducing the formation of fibrotic TME. Thus, inhibition of Wnt5a in BPD6 melanoma cells was found to boost the anti-tumor immune response of ICD inducers. Cationic lipid protamine NPs loaded with plasmid DNA encoding for the Wnt5a trap promoted the expression of Wnt5a trap leading to a powerful reduction of the tumoral Wnt5a level¹³⁷. When combined with low-dose DOX as an ICD inducer, Wnt5a trapping elicited

efficient innate and adaptive immune responses by remodeling the fibrotic immunosuppressive TME, recovering DC functions, and facilitating T cell infiltration resulting in tumor growth inhibition, survival prolongation and delayed tumor metastasis¹³⁷.

The upregulated Wnt ligands in the TME and TDLNs stimulates β -catenin signaling in DCs leading to enhanced secretion of retinoic acid (RA) and IL-10. The activated Wnt/ β -catenin signaling promotes Treg cell responses while dampens anti-tumor effector T cell responses resulting in immunosuppression^{138,139}. Therefore, the tankyrase inhibitor XAV939 was used to induce β -catenin degradation to enhance the antitumor immune response. Incorporation of XAV939 into d- α -tocopheryl polyethylene glycol 1000 succinate micelles significantly enhanced ICD of B16F10 mouse melanoma cells compared to free drug with a significant extracellular release or expression of HMGB1, CRT, and ATP¹⁴⁰. In a mouse model of conjunctival melanoma, local intra-tumoral delivery of XAV micelles significantly suppressed tumor progression through increased tumor cell ICD.

4.9.2. Zoledronic acid

Zoledronic acid (ZA), aminobisphosphonate drug, reverses chemo- and immune-resistance *in vitro*. Self-assembling NPs were prepared by mixing ZA complexed with calcium phosphate (CaP) NPs, with cationic liposomes¹⁴¹. The resultant NPs restored the DOX-induced ICD and reversed the tumor-mediated immunosuppression attributed to kynurenine production, by suppression of STAT3/IDO signaling. ZA also reduces expression of P-glycoprotein by inhibiting farnesyl pyrophosphate synthase in mevalonate pathway thus decreasing chemoresistance. This, consequently, increased the number of tumor infiltrating DCs while decreasing the number of immunosuppressive T-regs¹⁴¹. As a result, the NPs enhanced the sensitivity of chemo-immunoresistant tumors to DOX.

4.9.3. Formyl peptide receptor 1 (FPR-1) agonist

The formyl peptide receptor, in conjunction with its soluble ligand annexin A1 (secreted by cancer cells), orchestrates the chemotactic activity of DCs towards dying bodies, thus facilitating faster antigen processing and presentation¹⁴². The FPR-1 agonist WKYMVm was incorporated into peptide NPs together with cisplatin and Adjudin¹⁴³. While cisplatin and Adjudin induced ICD *via* ROS generation, WKYMVm could further trigger anti-TNBC immune response by activating FPR-1 which facilitates DCs to come close to dying cancer cells and consequently promote their interactions¹⁴³.

4.9.4. Tumor penetrating peptides

Co-administration of RGD (a tumor-penetrating peptide) with pirarubicin-encapsulated nanostructured lipid carriers enhanced drug tumor accumulation by increasing tumor vasculature extravasation and tumor tissue penetration¹⁴⁴. Without RGD, the NPs were located mostly around the tumor blood vessels. As a result, RGD both increased the drug cytotoxicity and enhanced its anti-tumor immune response in breast cancer bearing mice.

4.9.5. Aminoguanidine (AG)

AG was coupled to the surface of pH-responsive polymeric NPs loaded with bortezomib (BTZ)¹⁴⁵. While BTZ induced ICD of 4T1 breast cancer cells, the released AG stimulated TLR4 signaling thus enhanced the uptake of tumor antigens by DCs resulting in their maturation and consequently infiltration of CTLs in lymph nodes and tumors. Synergistic delivery of BTZ and AG

markedly suppressed 4T1 tumor and enhanced the α PD-L1 efficacy.

5. Recent trends in ICD inducing nanomedicines

5.1. ER-targeted PDT

Among PDT limitations, the short half-life and limited intracellular diffusion depth of ROS hinder its localization in the ER, thereby constraining the induction of ER stress. Targeted accumulation of the PS within ER leads to localized generation of high ROS level resulting in increased ER stress and hence more powerful ICD. Unlike hypericin, many PSs such as ICG are distributed to cytoplasm after internalization into cancer cells resulting in weak ICD induction. Therefore, ER-targeting par-daxin peptides were used for ER-targeted delivery of ICG-coupled hollow gold nanospheres. After internalization into CT-26 cells, the ER-targeted NPs accumulated into the ER compared to the non-targeted NPs which showed accumulation within lysosomes¹³⁰. Thus, the ER-targeted NPs showed higher intracellular stability against degradation by lysosomal enzymes. Upon exposure to NIR light, the ER-targeted NPs induced intense ROS-based ER stress as indicated by overexpression of the pro-apoptotic protein CHOP, an indicator of ER apoptosis¹³⁰. In addition, the resultant Ca^{2+} leakage triggered mitochondrial-related cell death, marked by elevated levels of cleaved caspase-3. In a similar vein, PEGylated lipid NPs encapsulating an ER-targeting photosensitizer TCPP, which selectively accumulates in the ER and generates ROS upon NIR laser irradiation, were synthesized¹⁴⁶. These NPs boosted ICD and stimulated immune cells, with increased secretion of HMGB1 and surface exposure of CRT. As a result, increased infiltrating CD8⁺ T cells and enhanced production of IL-12P40, TNF- α , and INF- γ in primary and distant tumors of irradiated mice treated with these NPs was observed¹⁴⁶.

5.2. Focused ultrasound (FUS) hyperthermia

Local stimulation of ICD by enhancing CRT expression in solid tumors is a promising strategy. Upon its translocation to cancer cell surface, CRT enhances phagocytosis of dying tumor cells by APCs. However, its rate and extent of expression showed high variability and usually not sufficient to elicit powerful antitumor immune response. Another interesting approach, FUS is a non-invasive extracorporeal strategy that uses focused sound waves to generate hyperthermia¹⁴⁷. The FUS-mediated thermal effect modulates the TME to increase responsiveness to cancer therapy by enhancing the release of TAAs, expression of Hsp, and up-regulation of pro-phagocytic CRT, resulting in improved antitumor immunity. To combine the benefits of both strategies, cationic liposomal CRT-NPs were developed by electrostatic complexation between cationic DOTAP and anionic CRT plasmid and then followed by FUS-induced hyperthermia¹⁴⁷. Intratumoral injection of CRT-NPs into B16 melanoma tumors followed by FUS heating (42–45 °C, around 15 min) resulted in enhanced CRT membrane expression and improved tumor antigen release thereby promoting ICD. The FUS/CRT liposomes resulted in >85% inhibition of melanoma growth which was 50% higher than with CRT-NPs or FUS alone. Knowing that CD47, don't eat me negative checkpoint that inhibits phagocytosis, counteracts the CRT pro-phagocytic action of melanoma cells¹⁴⁸, combination of FUS with CRT-NPs elevated CRT expression without markedly altering CD47

membrane expression. This led to a 1.5-fold rise in CRT/CD47 ratio and a 2-fold surge in the M1/M2 ratio compared to using CRT liposomes alone.

Another application of US waves involves decorating the surface of ultrasonic microbubbles (MBs) with DOX-loaded liposomes *via* avidin-biotin coupling¹⁴⁹. Application of high-intensity US resulted in inertial acoustic cavitation effects (sonoporation) which induced formation of transient pores in cell membrane thus triggered DOX release and enhanced its cellular uptake leading to high tumor accumulation with more DOX entered the nucleus. As a result, MB-DOX + US treatment resulted in enhanced ICD response in LL/2 and CT26 tumor models by inducing more ER stress-related release of DAMPs, such as CRT, ATP, and HMGB1¹⁴⁹.

5.3. Combined melanin/IDOi NPs

In contrast to the commonly used poorly biocompatible inorganic semiconductor phototherapy NPs, the natural pigment melanin NPs obtained from cuttlefish were developed as PTT reagents to induce ICD¹⁵⁰. As black materials, under 808 nm irradiation, the NPs could absorb all UV–Vis wavelengths exhibiting high PTT conversion capacity. To synergistically reverse the immunosuppressive TME, melanin NPs were loaded with IDO inhibitor INCB24360 to inhibit the tumor immune evasion¹⁵⁰. The NPs

efficiently enhanced the intratumoral infiltration of CTLs and increased the secretion of cytokines leading to suppression of both primary and abscopal distant tumors.

5.4. Cell membrane camouflaged NPs

A novel type of biomimetic NPs was developed by coating NPs with specific cell membranes. This approach combines the functional characteristics of cell membranes and the engineering versatility of synthetic nanocarriers and used mainly for prolongation of systemic circulation or cell-specific targeted drug delivery¹⁵¹. Coating of the Ce6-loaded magnetic mesoporous silica NPs with MCF-7 cancer cell membranes resulted in enhanced internalization into MCF-7 cells while reduced their phagocytic uptake into macrophages (Fig. 7A)⁹². This can be attributed to high expression of cell membrane protein CD47 thus increased their homologous tumor-targeted accumulation. The ROS generated by release of the PS Ce6 together with magnetic hyperthermia resulted in powerful ICD of MCF-7 cancer cells. Similarly, coating of melanin PTT NPs with membrane of 4T1 breast cancer cells could avoid immune clearance and promoted tumor homing characteristics¹⁵⁰.

Another approach used RBC's membrane for coating of hyaluronate-coated cationized BSA-stabilized gold nanoclusters to deliver PTX and PS PheoA⁹⁴. Expression of the anti-phagocytic

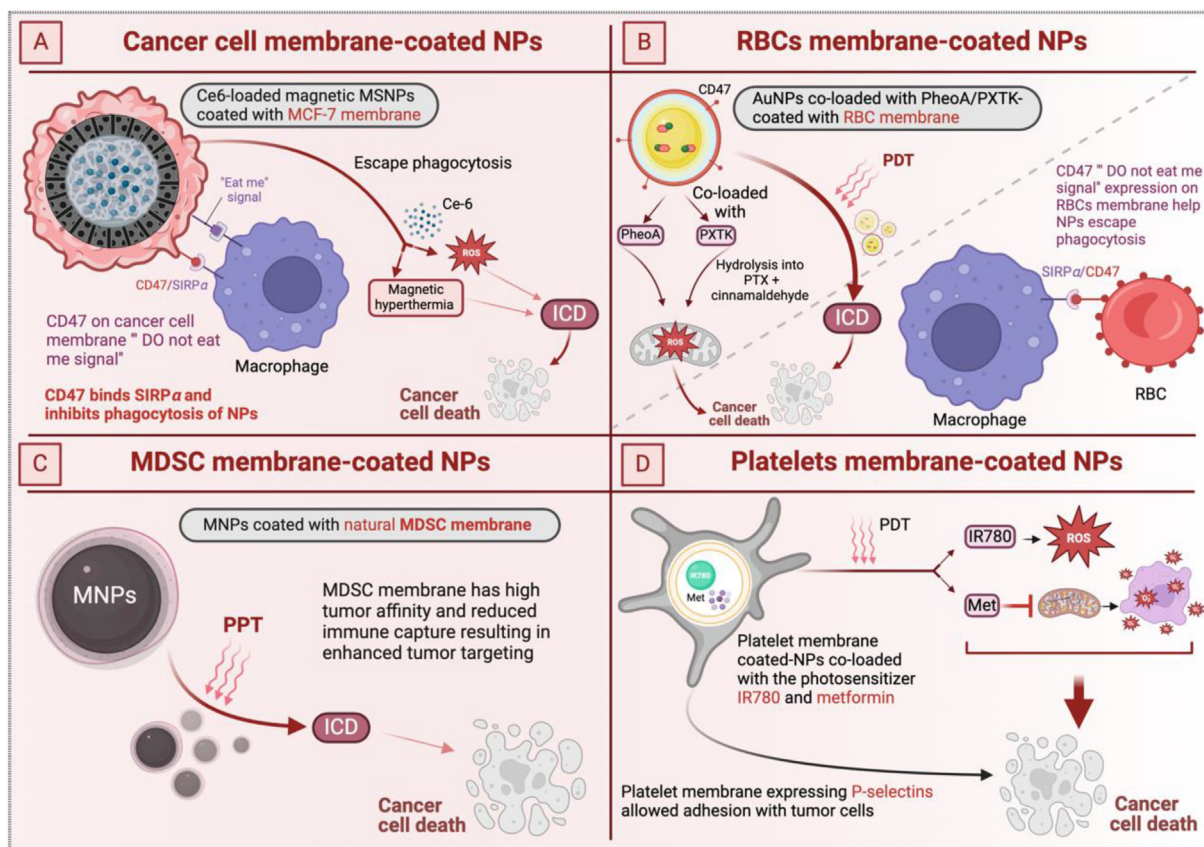


Figure 7 Cell membrane camouflaged nanomedicines used to boost the antitumor immunity of ICD inducers. (A) Breast cancer MCF-7 cell membrane used for coating of Ce6-loaded magnetic mesoporous silica NPs decreased elimination by macrophages due to upregulated CD47 thus enhanced their tumor accumulation⁹². (B) RBC membrane was used for coating of hyaluronate-coated cationized gold nanoclusters to prolong their circulation and tumor targeting⁹⁴. (C) MDSC membrane used for coating of MNPs inhibited their immune capture and increased their tumor accumulation⁶¹ and (D) platelet membrane (PM) used for coating PS IR780 and metformin co-loaded NPs increased their tumor accumulation by enhancing adhesion with cancer cells¹²⁹ (created *via* BioRender).

CD47 protein by RBC's membrane resulted in extended circulation (Fig. 7B). At TME, the original 150 nm size NPs were transformed into smaller size inner nanogold core upon hydrolysis of HA layer by hyaluronidase enzyme to enable their deep tumor penetration. Under laser irradiation, the combined chemotherapy/PDT-mediated ICD increased the tumor infiltrating CD8⁺ T cells resulting in 74.3% breast tumor growth inhibition and prevented pulmonary metastasis⁹⁴.

Due to their non-immunogenicity and high tumor affinity, coating of MNPs with natural MDSC membrane inhibited their immune capture and enhanced tumor targeting with higher efficiency compared to RBC's membrane-coated MNPs or naked MNPs (Fig. 7C)⁶¹. Further irradiation of MNPs with laser resulted in powerful PTT leading to ICD of melanoma cells with enhanced release of DAMPs thereby inhibited tumor growth in melanoma bearing mice⁶¹. Platelet membrane (PM), as a natural component of blood, was also used for coating NPs co-loaded with the PS IR780 and metformin enabling their escape from immune surveillance (Fig. 7D)¹²⁹. The PM expressed specific P-selectin proteins that allowed active adhesion between PM and tumor cells thus ensured tumor accumulation of IR780 and metformin resulting in a longer circulation lifetime¹²⁹.

5.5. Amplification of ICD cascade

The IDO-1 inhibitor, 1-MT was combined with Ce6 and α PD-L1 in NPs formed by self-assembly of hyaluronic acid and polylysine (Fig. 8)²⁴. Under NIR light irradiation, the NPs amplified the three

stages of cancer immunity cycle. Whereas Ce6 PDT-mediated ICD enhanced antigen presentation by DCs (phase I), 1-MT inhibited IDO1 and increased T cell proliferation (Phase II), and α PD-L1 suppressed PD-1/PD-L1 pathway to reactivate CTLs that kill cancer cells (Phase III). As a result, the NPs effectively elicited a powerful antitumor immunity and immune memory that suppressed tumor metastasis and relapse in B16F10 tumor-bearing mice²⁴. ICD could also be potentiated by amplifying ROS cascade. It was reported that cisplatin can generate ROS through activating NOXs, however; it does not elicit ICD by itself due to absence of CRT exposure. Adjuvin, a derivative of Isoniazid, was found to trigger apoptosis by enhancing intracellular ROS production. Therefore, for enhancing ICD response, cisplatin and adjuvin were co-incorporated into multi-responsive peptide-based NPs¹⁴³. The NPs synergistically amplified ROS cascade *via* enhancing the production of H₂O₂ and subsequent generation of highly toxic ROS like \cdot OH which triggered ER stress and induced powerful ICD response against TNBC demonstrated by surface expression of CRT and secretion of HMGB1 and ATP¹⁴³. Treatment with NPs resulted in 93.1% suppression of the growth of both primary tumor and lung metastasis with overall 82 days survival. Similarly, dihydroartemisinin (DHA) was combined with OXA in lipid NPs to amplify ROS and boost the ICD anti-tumor immune response⁸. DHA possesses an endoperoxide bridge that interacts with a ferrous iron catalyst to produce free radicals and cause oxidative stress. The generated ROS caused mitochondrial dysfunction with release of cytochrome *c*, disrupting the membrane potential. Moreover, the generated ROS could suppress

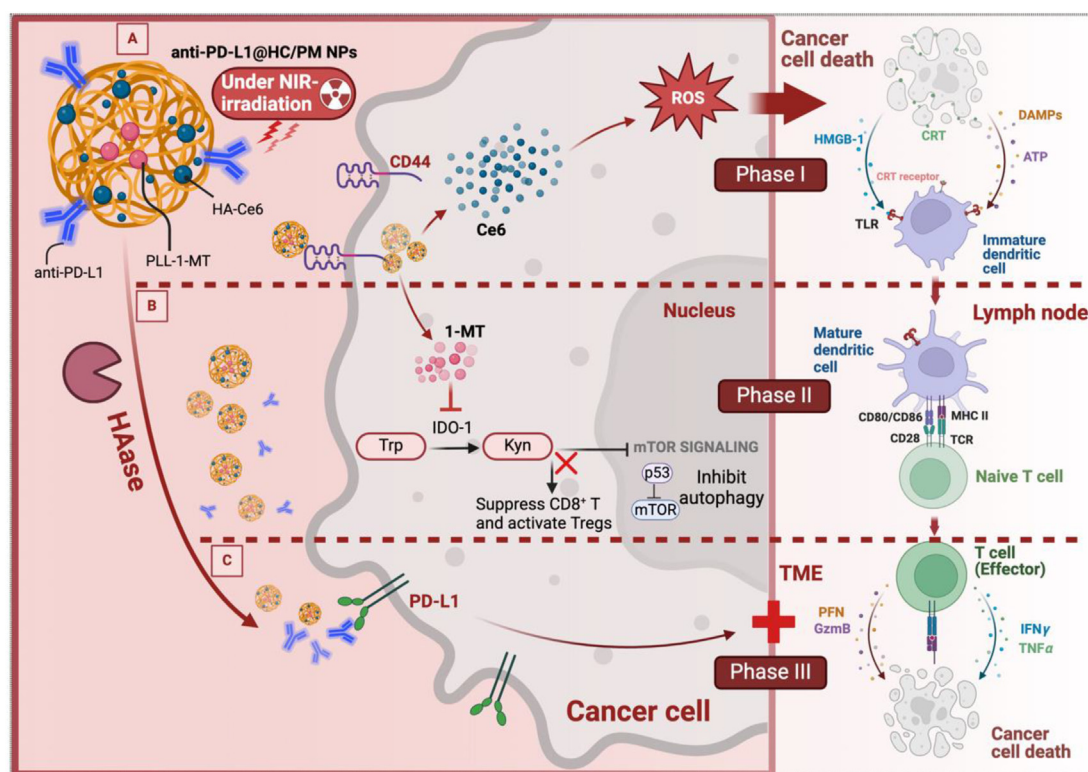


Figure 8 Amplification cascade of the cancer-immunity cycle *via* three-in-one immunomodulatory nanomedicines. The IDO-1 inhibitor, 1-MT was combined with Chlorin e6 (Ce6) and anti-PD-L1 into self-assembled hyaluronic acid and polylysine NPs²⁴. (A) Under NIR light irradiation, the NPs could amplify the three phases of cancer-immunity cycle, where Ce6 PDT-mediated ICD enhanced release of DAMPs and antigen presentation by DCs (Phase I), (B) 1-MT inhibits IDO and enhanced T cell proliferation (Phase II), and (C) anti-PD-L1 suppressed the PD-1/PD-L1 axis to reactivate cytotoxic T cells that kill cancer cells (phase III) (created *via* BioRender).

CT26 cell growth by G2/M phase cell cycle arrest *via* ER stress⁸. When combined with α PD-L1, OXA/DHA NP administration totally eradicated CRC tumors, and the treated mice remained tumor-free for about 4 months when re-challenged with live CT26 cancer cells.

5.6. Metallo-immunotherapy as ICD nanoamplifier

Silver NPs reduced using β -D-glucose were shown to interfere with cell cycle of MCF7 breast cancer cells leading to their death associated with release of DAMPs including Hsp70, Hsp90, HMGB1, and ATP along with CRT exposure¹⁵². However, immunization of mice with 4T1 cells treated with those NPs failed to induce a complete immune response *in vivo* where they did not prevent tumor development in re-challenge test. The authors attributed this partial response to the residual NPs present in the cells which could impair both the antigen presenting capacity of DCs and the lymphocyte ability to release granzyme B. Another study showed that diselenide-bridged mesoporous organosilica NPs (MONs) could promote ROS generation and ER stress thus potentiating ICD response¹⁵³. On the other hand, the metal-based chemotherapeutic ruthenium compound (KP1339) was characterized as an ICD inducer. Besides its unique redox properties, selenium (Se) was used to coordinate KP1339 to enable its controlled release *via* competitive coordination and matrix degradation in response to glutathione (GSH). High-dose of MONs selectively induced ROS generation while reduced the GSH levels resulting in oxidative ER stress, thus selectively killed tumor cells *via* amplified KP1339-mediated ICD immune response¹⁵³. When used in conjunction with PD-L1 checkpoint inhibitor, tumor cell membrane-coated MONs/KP1339 suppressed the growth of distant tumors and lung metastasis in mice bearing 4T1 orthotopic mammary tumors.

A metal-based copper(II) complex, containing a Schiff base ligand and a polypyridyl ligand, was reported to induce ICD of breast cancer stem cells (CSCs)¹⁵⁴. To enhance its stability, the Cu(II) complex was encapsulated into PEGylated PLGA NPs. The NPs enhanced the generation of intracellular ROS resulting in ER stress and release of DAMPs including CRT and HMGB1 along with ICD of breast CSCs¹⁵⁵. The NPs exhibited high cytotoxicity to both mammospheres, with 185-fold more than the known breast CSC killing drug salinomycin, and to bulk breast cancer cells and CSCs with low IC₅₀ value of 0.01 μ mol/L. In a progressive effort, Cu-based nanoscale coordination polymers (Cu-NCPs) were developed which enhanced the radiotherapy-mediated ICD of CT26 cells. A dual mechanism for the mixed-valence (Cu⁺/Cu²⁺) Cu-NCPs was proposed where Cu⁺ enhances generation of \cdot OH radicals from decomposition of the overexpressed H₂O₂ *via* Fenton Reaction to compensate the insufficient ROS generation by X-ray radiation¹⁵⁶. The second mechanism involves Cu²⁺-induced GSH elimination by converting GSH, acting as \cdot OH scavenger, to glutathione disulfide (GSSG). As a result, the NPs increased the infiltration of CD8⁺ T-cells in a CT26 bilateral tumor model, resulting in 25% complete eradication of nonirradiated tumors which was increased to 62.5% when combined with α PD-L1 therapy.

5.7. Endocellular ion nanomodulators

Recently, many inorganic nanomodulators including calcium (CaP, CaCO₃) and sodium chloride (NaCl) NPs have been developed for cancer therapy through ion overload-mediated ICD *via* disrupting

intracellular ion homeostasis. Potassium chloride NPs were encapsulated into cancer cell membrane-coated PLGA NPs. Once internalized by cancer cells, the NPs were degraded in acidic lysosomes, and released K⁺ and Cl⁻ ions which rapidly increased the osmotic pressure of 4T1 cancer cells resulting in their rupture and death¹⁵⁷. In addition, the NPs triggered release of ATP and HMGB1 from cancer cells together with surface expression of CRT which promoted DC maturation. In another investigation, Pt(IV) prodrugs were physically adsorbed and oxidatively polymerized in the pores of CaCO₃ NPs decorated with biotinylated PEGylated lipid to improve their aqueous solubility and tumor targeting. In the presence of tumoral acidity and GSH, the NPs were degraded into Ca²⁺ and cisplatin¹⁵⁸. The increased mitochondrial Ca²⁺ overload, leading to cytochrome C release and caspase 3 activation, GSH depletion, Pt-DNA crosslinking and excessive generation of ROS and lipid peroxide, resulted in ICD of cisplatin-resistant non-small lung cancer cells. Sodium citrate NPs enveloped in a phospholipid shell have also been exploited to induce ICD. These NPs disintegrate within cancer cells, subsequently releasing substantial concentrations of citrate and sodium ions¹⁵⁹. The elevated osmotic pressure inside the cell due to ion influx resulted in pyroptotic cell death mediated by caspase-1 and gasdermin D. Concurrently, the released citrate also stimulated the caspase-8/gasdermin C mediated pathway. The concurrent activation of these mechanisms resulted in pronounced ICD of 4T1 cells with release of CRT, HMGB1 and ATP and suppression of 4T1 tumor growth.

5.8. Hypoxia targeting bacteria

The lipopolysaccharides of the gram-negative bacteria (*e.g.*, *E. coli*) outer membrane nanovesicles can be taken up by circulating neutrophils and thus reach deep tumors. Furthermore, the bacterial abundant pathogen associated pattern molecules promote an antitumor immune response even in the immunosuppressive TME thus acting as immunoadjuvant^{160,161}. In the study of Liu et al.¹⁶², the bacterial outer membrane nanovesicles were used to modify the surface of Fe₃O₄-MnO₂ NPs in order to enhance their ICD response. In addition to the tumor PTT ablation mediated by the released iron and manganese ions, the inflammatory response induced by PTT effect enriches the tumor by neutrophils-packed NPs. The oxygen generated by MnO₂ NPs also helps overcome tumor hypoxia and immune resistance. Upon NIR irradiation, the intravenously administered bacterial camouflaged NPs markedly delayed the tumor growth of B16F10 tumor bearing mice. Inspired by their hypoxia targeting and hence deep tumor penetrating capacity, living anaerobic bacteria have been engineered with NPs for tumor delivery of various drugs and genes¹⁶³. The probiotic *Bifidobacterium bifidum* (Bi) was covalently coupled with DOX-loaded CaP/SiO₂ NPs. The Bi targeting hypoxic tumor markedly enhanced the cross-presentation of TAAs from B16F10 cells to DCs *via* Cx43-dependent gap junctions¹⁶⁴. Therefore, it enhanced the ICD inducing activity of DOX leading to DC maturation and infiltration of CD8⁺ T cells. This combined therapy suppressed the growth of primary murine B16F10 melanoma tumor and mitigated its metastatic dissemination.

5.9. Nanoscale metal-organic frameworks (NMOFs)

Nanoscale metal-organic frameworks (NMOFs) are a class of porous materials composed of metal ions or clusters coordinated to organic ligands to form one-, two-, or three-dimensional nanoscale structures. NMOFs themselves can induce ICD of

cancer cells and enhance antitumor immunity. Gd-MOF-5 NPs transported Gd^{3+} and Zn^{2+} into cancer cells causing Zn^{2+} overload which resulted in mitochondrial dysfunction and induced ER stress leading to ICD¹⁶⁵. As a result, the NPs showed elevated CRT surface exposure and release of HMGB1 and ATP. The NPs significantly suppressed the growth of 4T1 primary and distal tumor when combined with α PD-L1. Moreover, the highly surface area and porous structure of NMOF enables the delivery of different cargos that mediate ICD *via* chemo, PTT, PDT, CDT or radiotherapy¹⁶⁶.

5.10. GSH-depleting self-immolative polymers

The generated ROS by ICD inducers is eliminated by intracellular antioxidants like glutathione (GSH), resulting in impaired ER-stress. To potentiate its ICD inducing power, DOX was encapsulated into ROS-responsive self-immolative polymer-based micelles. In the presence of ROS, the polymer undergoes rapid depolymerization and released DOX that induced ICD of 4T1 cancer cells¹⁶⁷. Meanwhile, the resultant azaquinone methide derivatives, produced by self-immolation of the polymer efficiently depleted the intracellular GSH thus disrupting the redox homeostasis and augmenting the DOX induced ROS-based oxidative stress. As a result, the DOX-loaded polymer NPs promoted release of DAMPs and DC maturation in 4T1 tumor bearing mice with 1.74-fold higher tumor growth suppressing efficiency than DOX-treated tumor at the same dose.

5.11. Non-conventional unitized ICD nanoinducer

A non-conventional ICD inducer was developed by co-encapsulation of curcumin and iron oxide NPs into disulfide-bond incorporated dendritic mesoporous organosilica NPs¹⁶⁸. While curcumin induces ER stress by depleting Ca^{2+} and inhibition of thioredoxin reductase, iron oxide NPs showed a catalytic role in the Fenton reaction, and the disulfide bond structured NPs induced GSH depletion. As a result, the NPs triggered strong ICD and anticancer activity against 4T1 breast cancer cells *in vitro* and *in vivo* due to increased intracellular oxidative stress and ER stress. The NPs showed higher selectivity to cancer cells with significantly higher levels of thioredoxin reductase and H_2O_2 compared to normal cells. The NPs synergistically enhanced the antitumor efficacy of α PD-L1 therapy with 40% higher efficiency than combined DOX/ α PD-L1 therapy.

5.12. Integrated CD40L lipid NPs/CD40 DC therapy

CD40 and CD40 ligand (CD40L) are a pair of co-stimulatory molecules that belong to the tumor necrosis factor/tumor necrosis factor receptor family. To overcome the immunosuppressive TME, CD40 ligand mRNA-loaded lipid NPs were combined with DCs transfected with CD40 mRNA-loaded lipid NPs¹⁶⁹. First, the CD40L NPs triggered efficient ICD in tumoral tissues, along with release of TAAs and the expression of CD40 ligand by $CD4^+$ T cells. The ICD was denoted by increase in levels of extracellular HMGB1, extracellular ATP and cellular surface CRT in B16F10 cells by about 10-, 7- and 45-fold higher than non-treated cells, respectively. Then, CD40-transfected bone-marrow-derived dendritic cells (CD40-BMDCs) were intratumorally adoptively transferred and activated by the tumoral CD40 ligand molecules. As a result, the DCs capture TAAs leading to their maturation and secretion of proinflammatory cytokines IL-1 β , TNF α and IL-12

and upregulating the costimulatory molecules CD80 and CD86 by DCs resulting in reversal of the immunosuppressive TME. This led to successful presentation of TAAs by DCs to T cells and elicited T cell specific immune response which eliminated primary tumor and inhibited metastasis and relapse in B16F10 tumor model. Four doses of the combined CD40L-LNPs and adoptive CD40-BMDC transfer synergistically induced complete tumor regression in 83% of B16F10 tumor-bearing mice. Novel nanomedicine-based approaches for enhancing ICD of cancer cells are summarized in Table 2.

6. Challenges and future perspectives

Induction of ICD has shown a great promise in cancer immunotherapy mainly because of its success in eliciting systemic antitumor T cell response. However, the relatively weak and transient immune response unable to inhibit tumor recurrence in addition to the systemic adverse effects remain formidable challenges against clinical application of ICD inducers¹⁷⁰. While cytotoxic chemotherapeutics (such as DOX and MTX) and radiotherapy can provoke ICD, the response is usually weak since it is only mediated by secondary or collateral ER stress effects. To overcome this challenge, chemotherapy-induced ICD should be combined with more focused ROS-based ER stress inducing modality such as PDT. The immunogenicity accompanied by ICD, prompted by direct ROS-based ER stress, is more potent than that induced by secondary ER stress effects¹³⁰. However, PDT also has some disadvantages related to the inefficient tissue penetration of visible light, that severely limits the clinical application of PDT to superficial tumors. Moreover, PDT has low capacity to entirely kill malignant cells due to the tumor characteristic hypoxia at the core and usually ineffective against distant metastatic tumors⁸. In a similar vein, cancer immunotherapy based on photothermal ablation is hindered by limited laser penetration and inadequate stimulation of the ICD effect. To address these challenges, NIR-II light, which has a superior ability to penetrate tissue, was employed to enhance the PDT- and PTT-triggered ICD immune response. Although killing of cancer cells induced by RT is thought to be immunogenic and enhances the activity of CTLs to promote efficient systemic immune response, not all RT-induced modifications of the TME lead to immunostimulatory response. For example, the RT-triggered abscopal effect can be compromised by post-RT accumulation of the immunosuppressive protumorigenic M2 macrophages and Treg cells in hypoxic areas of irradiated tumors in addition to the immunosuppressive factors such as CD47 and PD-L1 upregulated by cancer cells. Therefore, the RT parameters should be controlled to identify the optimal dose and fractionation of RT and combination schedule with immunotherapy to amplify the antitumor immune response^{39,172}.

Currently, only few modalities have been proved to provoke ICD of tumor cells. In future studies, novel nanomedicine-based strategies to induce ICD should be investigated in order to elicit powerful long-lasting antitumor immune response without causing systemic toxicity. Moreover, advanced immunomodulatory modalities should be assessed to synergize with ICD inducers to enhance the outcomes of cancer immunotherapy. The treatment timing schedule, concomitant or sequential, of combination therapy between ICD inducers and synergistic immune checkpoint inhibitors or immunoadjuvants should be also investigated. Several drug candidates have been reported to induce or boost ICD antitumor immune response and therefore are good

Table 2 Novel nanomedicine-based approaches for enhancing ICD of cancer cells.

Nanoparticle type	Mechanism of ICD induction	Tumor model	Major outcome	Ref.
Pardaxin peptides modified ICG-coupled hollow gold nanospheres	ER-targeted PDT leads to accumulation of the PS within ER leading to localized generation of ROS resulting in increased ER stress and more powerful ICD.	CT-26 colorectal tumor model	Under NIR light, the NPs induced intense ROS-based ER stress. The resultant Ca^{2+} leakage triggered mitochondrial-related cell death & elevated cleaved caspase-3.	130
Cationic liposomal CRT plasmid NPs followed by FUS	FUS hyperthermia enhanced the release of TAAs, expression of Hsp, and upregulation of CRT, resulting in improved ICD immunity.	B16F10 melanoma model	FUS/CRT liposomes resulted in >85% inhibition of melanoma growth which was 50% higher than with CRT-NPs or FUS alone.	148
Copper sulfide (CuS) NPs under pulsed-wave laser	PW laser involves irradiation of cancer cells with short pulses that ablate tumor by a combined PTT and photomechanical effect termed photothermolysis.	B16-OVA mouse model	Under irradiation with 15-ns laser pulses, CuS NPs-mediated photothermolysis enhanced survival of mice re-challenged with tumor cells at a distant site.	170
Ferrimagnetic vortex-domain iron oxide (FVIOs) nanorings	Under AMF, FVIO-mediated mild hyperthermia triggers apoptosis and CRT exposure on cancer cells, thereby enhancing phagocytic uptake & triggering powerful ICD.	4T1 breast cancer cells	This mild thermotherapy induced an 88% enhancement in CTL infiltration in distant tumors and suppresses the activity of myeloid-derived suppressor cells (MDSCs).	72
Cu-based coordination polymer NPs	Cu^{+} enhances generation of hydroxyl radicals $\cdot OH$ via Fenton reaction, Cu^{2+} induces GSH elimination.	CT26 bilateral tumor model	The NPs resulted in 25% complete eradication of nonirradiated tumors which was increased to 62.5% when combined with $\alpha PD-L1$.	157
Bacterial outer membrane-coated Fe_3O_4 - MnO_2 NPs	Bacterial pathogen associated pattern molecules promote an immune response. PTT ablation by the released iron & manganese ions.	B16F10 melanoma model	Upon NIR irradiation, the bacterial camouflaged NPs markedly delayed the tumor growth of B16F10 tumor bearing mice.	163
KCl NPs encapsulated into cancer cell membrane coated PLGA NPs	The released K^{+} and Cl^{-} ions increased osmotic pressure of cancer cells resulting in rupture and ICD with release of DAMPs.	4T1 breast cancer cells	Combination of KCl NPs with anti-PD-L1 antibodies suppressed growth of 4T1 tumor bearing mice.	158
Gd-MOF-5 NPs	The NPs transported Gd^{3+} and Zn^{2+} into cancer cells causing Zn^{2+} overload resulting in mitochondrial dysfunction and ER stress leading to ICD augmented response.	4T1 primary and distal tumor model	The NPs significantly suppressed the growth of 4T1 primary and distal tumor when combined with aPD-L1.	166
DOX-loaded ROS-responsive self-immolative polymer-based micelles	Azaquinone methide produced by the self-immolation of the polymer depleted the intracellular GSH thus augmenting DOX induced ROS-based oxidative stress.	4T1 tumor bearing mice	DOX-loaded polymer NPs resulted in 1.74-fold higher tumor growth suppressing efficiency than free DOX-treated 4T1 tumor bearing mice.	168
Curcumin and iron oxide NPs co-loaded disulfide-bond mesoporous organosilica NPs	ER stress by depleting Ca^{2+} and inhibition of thioredoxin reductase, Fenton reaction, and disulfide bond-induced GSH depletion.	4T1 breast cancer cells	The NPs showed higher selectivity to cancer cells compared to normal cells. Combined NPs & aPDL1 showed 40% higher efficiency than DOX/aPDL1 therapy.	169
RGD & TPP modified superparamagnetic NPs	Magnetic hyperthermia induces mitochondrial heat stress & intramitochondrial ROS generation thereby enhancing ICD response.	Hepa 1–6 hepatoma cells	Repolarizing the pro-tumorigenic M2 macrophages into anti-tumor M1 phenotype and increased its phagocytosis of cancer cells.	71
CD40L mRNA lipid NPs & DCs transfected with CD40 mRNA-loaded lipid NPs	CD40L NPs triggered efficient ICD along with release of TAAs and expression of CD40 ligand by $CD4^{+}$ T cells to activate DCs.	B16F10 melanoma model	The NPs plus adoptive transfer of DCs resulted in complete tumor regression in 83% of B16F10 tumor-bearing mice.	171

Table 3 Comparison of different ICD inducer strategies.

ICD inducer strategy	ICD mechanism	Advantage	Limitation	Example	Ref.
Chemo-therapy	Induces apoptosis by targeting DNA, cytosolic or membrane proteins. Causes ER stress as a secondary effect leading to release of DAMPs to stimulate immunity.	Efficient apoptosis, well-established method with known efficacy. Can be combined with other therapies.	Causes significant side effects; resistance development; ICD response is weak & transient since it is only mediated by collateral ER stress.	Doxorubicin Mitoxantrone Oxaliplatin	172,177,178
Radio-therapy (RT)	Ionizing radiation generates hydroxyl radical ($\cdot\text{OH}$) to induce damage of the tumor cellular components, including DNA, proteins, and membranes.	Well-established; induces a systemic immune response that affects distant tumor <i>via</i> abscopal effect.	Development of radio-resistance, post-RT accumulation of immunosuppressive M2 macrophages and Treg cells in hypoxic areas of irradiated tumors.	X-ray radiation	179–182
Photo-dynamic therapy (PDT)	The light-sensitive photosensitizers, upon activation by specific wavelengths of light, produces ROS that can induce ICD.	Minimally invasive; can be targeted specifically to tumor sites; reduced systemic toxicity.	Limited penetration depth of light; produces hypoxia; depends on oxygen concentration; not effective for distant tumors; high-light dose phototoxicity.	Photo-sensitizers like Chlorine e6 Pheophorbide A	183–185
Photo-thermal therapy (PTT)	PTT uses photothermal agents that absorb and convert light energy into heat, causing localized hyperthermia that can induce ICD.	Targeted therapy with minimal damage to surrounding tissues; can be combined with imaging for precise treatment.	Limited laser penetration; requires adequate light absorption; heat dissipation can be challenging; thermal damage to surrounding tissues.	Gold nanorods	60,62,137
Magnetic hyper-thermia	This approach uses magnetic nanoparticles that, when exposed to an alternating magnetic field, generate heat and induce hyperthermia-driven ICD.	Non-invasive; safe where it generates mild hyperthermia, thereby selectively killing tumor cells, has higher tissue penetration so can target deep tissues; ferroptotic agents can trigger an unfolded protein response and ER stress.	Requires precise temperature control; overheating causes damage to healthy tissues, insufficient heating may not induce ICD; efficacy diminishes with tumor depth due to reduced magnetic field strength; non-specific distribution of MNPs; off-target effects.	Iron oxide NPs	66,67,186
Chemo-dynamic therapy (CDT)	Utilizes Fenton or Fenton-like reactions to generate hydroxyl radicals from hydrogen peroxide present in the TME, inducing ICD.	Can specifically target TME; minimal invasiveness; generates highly reactive and toxic hydroxyl radicals; minimal systemic toxicity; potential for real-time imaging and monitoring.	TME characteristics as low pH, hypoxia, and high GSH levels can affect Fenton reaction and thus the efficiency of ROS generation; Non-specific distribution of NPs can result in off-target effects and damage to normal	Iron and manganese-based NPs	187,188

(continued on next page)

Table 3 (continued)

ICD inducer strategy	ICD mechanism	Advantage	Limitation	Example	Ref.
Sono-dynamic therapy (SDT)	Uses low intensity ultrasound to activate sonosensitizers, producing ROS and causing ICD.	Non-invasive; tumor selective; less dependent on oxygen presence; US waves can penetrate deeper into tissues compared to light; suitable for deep-seated tumors; lower side effects compared to radiation.	Requires appropriate sonosensitizers; US penetration depth and intensity can be limiting factors since its effectiveness still diminishes with depth, and the energy can attenuate in dense or heterogeneous tissues.	Sonosensitizer agents like Hematoporphyrin	74,189
Oncolytic therapy	Oncolytic peptides and viruses cause lysis of cancer cells with release of DAMPs that induce ICD of cancer cells.	Selective to tumor cells; can be effective against tumors resistant to chemo- and radiotherapy.	Instability of oncolytic peptides; short half-life; delivery challenges; resistance development.	Oncolytic peptides like LTX-315	80

candidates for nanomedicine-based combined delivery with conventional ICD inducers, immune checkpoint inhibitors or immunoadjuvants.

For example, CBP501, a calmodulin-binding peptide, was found to synergistically enhance ICD in combination with low dose of cisplatin as denoted by upregulation of ICD markers¹⁷³. In another study, blocking of Rho-kinase (ROCK) pathway resulted in enhanced phagocytosis of cancer cells and improved T cell priming by DCs. Combination of ROCK inhibitors with immunogenic chemotherapy synergistically enhanced DC maturation and CTL infiltration into tumors resulting in inhibited tumor growth in syngeneic tumor models¹⁷⁴. Similar ICD inducing effects were reported for the histone deacetylase inhibitor, vorinostat¹⁷⁵ and the cyclin-dependent kinase inhibitor, dinaciclib¹⁷⁶. Based on the promising potential of those drug candidates, nanomedicines can be developed to enable systemic delivery of those drug alone or in combination with conventional ICD inducers and immune checkpoint blockers such as anti-CTLA4 antibodies to boost the ICD immune response and boost the antitumor immunity. Combination of ICD inducing drugs with TME reprogramming strategies can be also evaluated. For example, drugs act by inducing quiescence of the immunosuppressive cancer associated fibroblasts, drugs that suppress the activity or infiltration of the immunosuppressive Tregs or MDSCs can be good candidates for combination with ICD inducers *via* nanomedicine platforms to boost their immunogenic response. Comparison of different ICD inducer strategies are summarized in Table 3^{60,62,66,67,74,80,172,177–189}.

Currently, a number of clinical trials are undergoing to evaluate the therapeutic and immunological efficacy of ICD-inducing chemotherapeutics, *e.g.*, DOX, MTX, OXA, cyclophosphamide, epirubicin, idarubicin, bleomycin, and bortezomib¹⁸⁹. Furthermore, the use of MNPs-based thermotherapy has gained approval from European regulatory authorities for treating glioblastoma multiforme and is currently undergoing phase II trials for prostate cancer treatment. Regarding future development directions and rational design of ICD-inducing nanomedicines, we propose several key factors for consideration. First, the design should focus on enhancing the specificity and targeting efficiency of nanomedicines to tumor cells, minimizing off-target effects and systemic toxicity. This can be achieved through surface modifications with ligands that bind specifically to receptors overexpressed on tumor cells. Second, the stability and controlled release of the therapeutic payload in the TME are crucial. Engineering nanomedicines for stimuli-responsive release, such as pH-sensitive or enzyme-triggered mechanisms, can improve the therapeutic efficacy and reduce side effects. Third, the immunological properties of the nanocarriers themselves should be considered; materials that inherently provoke an immune response or can be modified to do so may augment the overall ICD effect. Fourth, a multimodal approach combining different therapeutic strategies, such as chemotherapy, PDT, or radiotherapy with immunotherapy, should be explored to synergistically enhance ICD. This approach can leverage the unique advantages of each modality while overcoming their individual limitations. Finally, the development of these nanomedicines must be guided by a thorough understanding of the TME, including its hypoxic nature, immune cell infiltration, and extracellular matrix composition. Designing nanomedicines that can adapt to or modulate these conditions will be a significant step forward. As we advance, it is imperative to continuously integrate insights

from clinical feedback and emerging research to refine these designs, ultimately paving the way for more effective and personalized cancer therapies.

Overall, more work is required to identify new ICD inducing compounds or strategies and also to understand the synergistic immune mechanisms of the new combinatorial approaches and their impact on the immune response and TME. As a success parameter, the effective ICD inducing strategy should achieve stronger tumor growth inhibitory effect of established tumor in immunocompetent than in immunodeficient mice. Second, if injected subcutaneously, the ICD inducer drug-treated dying cancer cells should suppress the tumor growth in immunocompetent mice when re-challenged with live tumor cells.

Author contributions

Ahmed O. Elzoghby conceptualized the review idea and provided overall direction for the article. All of the authors contributed to writing the article. All of the authors have read and approved the final manuscript.

Conflicts of interest

The authors declare no conflicts of interest.

References

- Duan X, Chan C, Lin W. Nanoparticle-mediated immunogenic cell death enables and potentiates cancer immunotherapy. *Angew Chem Int Ed Engl* 2019;**58**:670–80.
- Kraehenbuehl L, Weng CH, Eghbali S, Wolchok JD, Merghoub T. Enhancing immunotherapy in cancer by targeting emerging immunomodulatory pathways. *Nat Rev Clin Oncol* 2021;**19**:37–50.
- Chow A, Perica K, Klebanoff CA, Wolchok JD. Clinical implications of T cell exhaustion for cancer immunotherapy. *Nat Rev Clin Oncol* 2022;**19**:775–90.
- O'Donnell JS, Teng MWL, Smyth MJ. Cancer immunoediting and resistance to T cell-based immunotherapy. *Nat Rev Clin Oncol* 2019;**16**:151–67.
- Kroemer G, Galassi C, Zitvogel L, Galluzzi L. Immunogenic cell stress and death. *Nat Immunol* 2022;**23**:487–500.
- Gao J, Wang WQ, Pei Q, Lord MS, Yu HJ. Engineering nanomedicines through boosting immunogenic cell death for improved cancer immunotherapy. *Acta Pharmacol Sin* 2020;**41**:986–94.
- Yang S, Sun IC, Hwang HS, Shim MK, Yoon HY, Kim K. Rediscovery of nanoparticle-based therapeutics: boosting immunogenic cell death for potential application in cancer immunotherapy. *J Mater Chem B* 2021;**9**:3983–4001.
- Duan X, Chan C, Han W, Guo N, Weichselbaum RR, Lin W. Immunostimulatory nanomedicines synergize with checkpoint blockade immunotherapy to eradicate colorectal tumors. *Nat Commun* 2019;**10**:1–15.
- Zhao X, Yang K, Zhao R, Ji T, Wang X, Yang X, et al. Inducing enhanced immunogenic cell death with nanocarrier-based drug delivery systems for pancreatic cancer therapy. *Biomaterials* 2016;**102**:187–97.
- Bezu L, Gomes-de-Silva LC, Dewitte H, Breckpot K, Fucikova J, Spisek R, et al. Combinatorial strategies for the induction of immunogenic cell death. *Front Immunol* 2015;**6**:187.
- Kepp O, Pol J, Zitvogel L, Kroemer G. Immunogenic stress and death of cancer cells in natural and therapy-induced immunosurveillance. *Oncol Immunology* 2017:215–29.
- Zhou J, Wang G, Chen Y, Wang H, Hua Y, Cai Z. Immunogenic cell death in cancer therapy: present and emerging inducers. *J Cell Mol Med* 2019;**23**:4854–65.
- Galluzzi L, Buqué A, Kepp O, Zitvogel L, Kroemer G. Immunological effects of conventional chemotherapy and targeted anticancer agents. *Cancer Cell* 2015;**28**:690–714.
- Garg AD, Agostinis P. ER stress, autophagy and immunogenic cell death in photodynamic therapy-induced anti-cancer immune responses. *Photochem Photobiol Sci* 2014;**13**:474–87.
- Jin MZ, Wang XP. Immunogenic cell death-based cancer vaccines. *Front Immunol* 2021;**12**:697964.
- Pierce RH, Campbell JS, Pai SI, Brody JD, Kohrt HE. *In-situ* tumor vaccination: bringing the fight to the tumor. *Hum Vaccines Immunother* 2015;**11**:1901–9.
- Hammerich L, Binder A, Brody JD. *In situ* vaccination: cancer immunotherapy both personalized and off-the-shelf. *Mol Oncol* 2015;**9**:1966–81.
- Marabelle A, Kohrt H, Caux C, Levy R. Intratumoral immunization: a new paradigm for cancer therapy. *Clin Cancer Res* 2014;**20**:1747–56.
- González FE, Gleisner A, Falcón-Beas F, Osorio F, López MN, Salazar-Onfray F. Tumor cell lysates as immunogenic sources for cancer vaccine design. *Hum Vaccines Immunother* 2014;**10**:3261–9.
- Wen Y, Chen X, Zhu X, Gong Y, Yuan G, Qin X, et al. Photothermal-chemotherapy integrated nanoparticles with tumor microenvironment response enhanced the induction of immunogenic cell death for colorectal cancer efficient treatment. *ACS Appl Mater Interfaces* 2019;**11**:43393–408.
- An M, Yu C, Xi J, Reyes J, Mao G, Wei WZ, et al. Induction of necrotic cell death and activation of STING in the tumor microenvironment via cationic silica nanoparticles leading to enhanced antitumor immunity. *Nanoscale* 2018;**10**:9311–9.
- Irvine DJ, Dane EL. Enhancing cancer immunotherapy with nanomedicine. *Nat Rev Immunol* 2020;**20**:321–34.
- Feng B, Zhou F, Hou B, Wang D, Wang T, Fu Y, et al. Binary cooperative prodrug nanoparticles improve immunotherapy by synergistically modulating immune tumor microenvironment. *Adv Mater* 2018;**30**:e1803001.
- Li Q, Zhang D, Zhang J, Jiang Y, Song A, Li Z, et al. A three-in-one immunotherapy nanoweapon via cascade-amplifying cancer-immunity cycle against tumor metastasis, relapse, and postsurgical regrowth. *Nano Lett* 2019;**19**:6647–57.
- Ma Y, Zhang Y, Li X, Zhao Y, Li M, Jiang W, et al. Near-infrared II phototherapy induces deep tissue immunogenic cell death and potentiates cancer immunotherapy. *ACS Nano* 2019;**13**:11967–80.
- Pan J, Hu P, Guo Y, Hao J, Ni D, Xu Y, et al. Combined magnetic hyperthermia and immune therapy for primary and metastatic tumor treatments. *ACS Nano* 2020;**14**:1033–44.
- Wang H, Tang Y, Fang Y, Zhang M, Wang H, He Z, et al. Reprogramming tumor immune microenvironment (TIME) and metabolism via biomimetic targeting codelivery of shikonin/JQ1. *Nano Lett* 2019;**19**:2935–44.
- Chen Q, Chen J, Yang Z, Xu J, Xu L, Liang C, et al. Nanoparticle-enhanced radiotherapy to trigger robust cancer immunotherapy. *Adv Mater* 2019;**31**:e1802228.
- Li Z, Chu Z, Yang J, Qian H, Xu J, Chen B, et al. Immunogenic cell death augmented by manganese zinc sulfide nanoparticles for metastatic melanoma immunotherapy. *ACS Nano* 2022;**16**:15471–83.
- Ding M, Zhang Y, Yu N, Zhou J, Zhu L, Wang X, et al. Augmenting immunogenic cell death and alleviating myeloid-derived suppressor cells by sono-activatable semiconducting polymer nanoparticles for immunotherapy. *Adv Mater* 2023;**35**:e2302508.
- Xia Y, Wei J, Zhao S, Guo B, Meng F, Klumperman B, et al. Systemic administration of polymersomal oncolytic peptide LTX-315 combining with CpG adjuvant and anti-PD-1 antibody boosts immunotherapy of melanoma. *J Control Release* 2021;**336**:262–73.
- Chang CL, Hsu YT, Wu CC, Lai YZ, Wang C, Yang YC, et al. Dose-dense chemotherapy improves mechanisms of antitumor immune response. *Cancer Res* 2013;**73**:119–27.
- Maeda H, Nakamura H, Fang J. The EPR effect for macromolecular drug delivery to solid tumors: improvement of tumor uptake,

- lowering of systemic toxicity, and distinct tumor imaging *in vivo*. *Adv Drug Deliv Rev* 2013;**65**:71–9.
34. Yin Y, Hu Q, Xu C, Qiao Q, Qin X, Song Q, et al. Co-delivery of doxorubicin and interferon- γ by thermosensitive nanoparticles for cancer immunochemotherapy. *Mol Pharm* 2018;**15**:4161–72.
 35. Kuai R, Yuan W, Son S, Nam J, Xu Y, Fan Y, et al. Elimination of established tumors with nanodisc-based combination chemo-immunotherapy. *Sci Adv* 2018;**4**:eaao1736.
 36. Matria EM, Cai LY, Kan MJ, Li X, Schaal JL, Fiering S, et al. Nanoparticle formulation improves doxorubicin efficacy by enhancing host antitumor immunity. *J Control Release* 2018;**269**: 364–73.
 37. Matha K, Lollo G, Taurino G, Respaud R, Marigo I, Shariati M, et al. Bioinspired hyaluronic acid and polyarginine nanoparticles for DACHPt delivery. *Eur J Pharm Biopharm* 2020;**150**:1–13.
 38. Fan Y, Kuai R, Xu Y, Ochyl LJ, Irvine DJ, Moon JJ. Immunogenic cell death amplified by co-localized adjuvant delivery for cancer immunotherapy. *Nano Lett* 2017;**17**:7387–93.
 39. Walle T, Martinez Monge R, Cerwenka A, Ajona D, Melero I, Lecanda F. Radiation effects on antitumor immune responses: current perspectives and challenges. *Ther Adv Med Oncol* 2018;**10**: 1758834017742575.
 40. Colton M, Cheadle EJ, Honeychurch J, Illidge TM. Reprogramming the tumour microenvironment by radiotherapy: implications for radiotherapy and immunotherapy combinations. *Radiat Oncol* 2020; **15**:254.
 41. Zitvogel L, Kroemer GJBCD. Bortezomib induces immunogenic cell death in multiple myeloma. *Blood Cancer Discov* 2021;**2**:405–7.
 42. Liu P, Zhao L, Pol J, Levesque S, Petrazzuolo A, Pfirschke C, et al. Crizotinib-induced immunogenic cell death in non-small cell lung cancer. *Nat Commun* 2019;**10**:1486.
 43. Petrazzuolo A, Perez-Lanzon M, Liu P, Maiuri MC, Kroemer G. Crizotinib and ceritinib trigger immunogenic cell death *via* on-target effects. *OncImmunology* 2021;**10**:1973197.
 44. Tseng LM, Lau KY, Chen JL, Chu PY, Huang TT, Lee CH, et al. Regorafenib induces damage-associated molecular patterns, cancer cell death and immune modulatory effects in a murine triple negative breast cancer model. *Exp Cell Res* 2023;**429**:113652.
 45. Liu CY, Lau KY, Huang TT, Chen JL, Chu PY, Huang CT, et al. Abstract P3-05-19: regorafenib induces immunogenic cell death *via* p-stat3 inhibition in triple negative breast cancer cells. *Cancer Res* 2018;**78**. P3-05-19-P3-05-19.
 46. Chen HM, Wang PH, Chen SS, Wen CC, Chen YH, Yang WC, et al. Shikonin induces immunogenic cell death in tumor cells and enhances dendritic cell-based cancer vaccine. *Cancer Immunol Immunother* 2012;**61**:1989–2002.
 47. Yang NS, Lin TJJR, Investigation C. Molecular basis of shikonin-induced immunogenic cell death: insights for developing cancer therapeutics. *Recep Clin Invest* 2016;**3**:e1234.
 48. Guo ZS, Kalinski P, Chen H, Zhu Z. Immunogenic cell death-inducing small molecule inhibitors: potential for immunotherapy of cancer. *Clin Transl Discov* 2022;**2**:e69.
 49. Zhai J, Gu X, Liu Y, Hu Y, Jiang Y, Zhang ZJFiP. Chemotherapeutic and targeted drugs-induced immunogenic cell death in cancer models and antitumor therapy: an update review. *Front Pharmacol* 2023;**14**: 1152934.
 50. Zitvogel L, Kroemer G. Bortezomib induces immunogenic cell death in multiple myeloma. *Blood Cancer Discov* 2021;**2**:405–7.
 51. Wang R, Xu X, Li D, Zhang W, Shi X, Xu H, et al. Smart pH-responsive polyhyalazine/bortezomib nanoparticles for remodeling tumor microenvironment and enhancing chemotherapy. *Biomaterials* 2022;**288**:121737.
 52. Petrazzuolo A, Perez-Lanzon M, Martins I, Liu P, Kepp O, Minard-Colin V, et al. Pharmacological inhibitors of anaplastic lymphoma kinase (ALK) induce immunogenic cell death through on-target effects. *Cell Death Dis* 2021;**12**:713.
 53. Liang Q, Lan Y, Li Y, Cao Y, Li J, Liu Y. Crizotinib prodrug micelles co-delivered doxorubicin for synergistic immunogenic cell death induction on breast cancer chemo-immunotherapy. *Eur J Pharm Biopharm* 2022;**177**:260–72.
 54. Lin TJ, Lin HT, Chang WT, Mitapalli SP, Hsiao PW, Yin SY, et al. Shikonin-enhanced cell immunogenicity of tumor vaccine is mediated by the differential effects of DAMP components. *Mol Cancer* 2015;**14**:174.
 55. Li J, Zhao M, Sun M, Wu S, Zhang H, Dai Y, et al. Multifunctional nanoparticles boost cancer immunotherapy based on modulating the immunosuppressive tumor microenvironment. *ACS Appl Mater Interfaces* 2020;**12**:50734–47.
 56. Li J, Zhao M, Xu Y, Hu X, Dai Y, Wang D. Hybrid micelles code-livering shikonin and IDO-1 siRNA enhance immunotherapy by remodeling immunosuppressive tumor microenvironment. *Int J Pharm* 2021;**597**:120310.
 57. Alzeibak R, Mishchenko TA, Shilyagina NY, Balalaeva IV, Vedunova MV, Krysko DV. Targeting immunogenic cancer cell death by photodynamic therapy: past, present and future. *J Immunother Cancer* 2021;**9**:e001926.
 58. Jin F, Liu D, Xu X, Ji J, Du Y. Nanomaterials-based photodynamic therapy with combined treatment improves antitumor efficacy through boosting immunogenic cell death. *Int J Nanomed* 2021;**16**: 4693–712.
 59. Song W, Kuang J, Li CX, Zhang M, Zheng D, Zeng X, et al. Enhanced immunotherapy based on photodynamic therapy for both primary and lung metastasis tumor eradication. *ACS Nano* 2018;**12**: 1978–89.
 60. Sweeney EE, Cano-Mejia J, Fernandes R. Photothermal therapy generates a thermal window of immunogenic cell death in neuroblastoma. *Small* 2018;**14**:e1800678.
 61. Yu GT, Rao L, Wu H, Yang LL, Bu LL, Deng WW, et al. Myeloid-derived suppressor cell membrane-coated magnetic nanoparticles for cancer theranostics by inducing macrophage polarization and synergizing immunogenic cell death. *Adv Funct Mater* 2018;**28**:1801389.
 62. Huff ME, Gökmen FÖ, Barrera JS, Lara EJ, Tunnell J, Irvin J, et al. Induction of immunogenic cell death in breast cancer by conductive polymer nanoparticle-mediated photothermal therapy. *ACS Appl Polym Mater* 2020;**2**:5602–20.
 63. Xiang H, Zhao L, Yu L, Chen H, Wei C, Chen Y, et al. Self-assembled organic nanomedicine enables ultrastable photo-to-heat converting theranostics in the second near-infrared biowindow. *Nat Commun* 2021;**12**:218.
 64. Xu H, Deng H, Ma X, Feng Y, Jia R, Wang Y, et al. NIR-II-absorbing diimmonium polymer agent achieves excellent photothermal therapy with induction of tumor immunogenic cell death. *J Nanobiotechnol* 2023;**21**:1–11.
 65. Cao Q, Wang W, Zhou M, Huang Q, Wen X, Zhao J, et al. Induction of antitumor immunity in mice by the combination of nanoparticle-based photothermolysis and anti-PD-1 checkpoint inhibition. *Nanomed Nanotechnol Biol Med* 2020;**25**:102169.
 66. Sato I, Umemura M, Mitsudo K, Kioi M, Nakashima H, Iwai T, et al. Hyperthermia generated with ferucarbotran (Resovist[®]) in an alternating magnetic field enhances cisplatin-induced apoptosis of cultured human oral cancer cells. *J Physiol Sci* 2014;**64**:177–83.
 67. Maier-Hauff K, Ulrich F, Nestler D, Niehoff H, Wust P, Thiesen B, et al. Efficacy and safety of intratumoral thermotherapy using magnetic iron-oxide nanoparticles combined with external beam radiotherapy on patients with recurrent glioblastoma multiforme. *J Neuro Oncol* 2011;**103**:317–24.
 68. Hoebe RA, Van Oven CH, Gadella Jr TW, Dhonukshe PB, Van Noorden CJ, Manders EM. Controlled light-exposure microscopy reduces photobleaching and phototoxicity in fluorescence live-cell imaging. *Nat Biotechnol* 2007;**25**:249–53.
 69. Mou Y, Wang J, Wu J, He D, Zhang C, Duan C, et al. Ferroptosis, a new form of cell death: opportunities and challenges in cancer. *J Hematol Oncol* 2019;**12**:34.
 70. Tang D, Kepp O, Kroemer G. Ferroptosis becomes immunogenic: implications for anticancer treatments. *OncImmunology* 2021;**10**: 1862949.

71. Jiang H, Fu H, Guo Y, Hu P, Shi JL. Evoking tumor associated macrophages by mitochondria-targeted magnetothermal immunogenic cell death for cancer immunotherapy. *Biomaterials* 2022;**289**:121799.
72. Liu X, Zheng J, Sun W, Zhao X, Li Y, Gong N, et al. Ferrimagnetic vortex nanoring-mediated mild magnetic hyperthermia imparts potent immunological effect for treating cancer metastasis. *ACS Nano* 2019;**13**:8811–25.
73. Tian Q, Xue F, Wang Y, Cheng Y, An L, Yang S, et al. Recent advances in enhanced chemodynamic therapy strategies. *Nano Today* 2021;**39**:101162.
74. Wang T, Peng W, Du M, Chen Z. Immunogenic sonodynamic therapy for inducing immunogenic cell death and activating antitumor immunity. *Front Oncol* 2023;**13**:1167105.
75. Wu T, Liu Y, Cao Y, Liu Z. Engineering macrophage exosome disguised biodegradable nanoplatform for enhanced sonodynamic therapy of glioblastoma. *Adv Mater* 2022;**34**:e2110364.
76. Zheng Y, Li X, Dong C, Ding L, Huang H, Zhang T, et al. Ultrasound-augmented nanocatalytic ferroptosis reverses chemotherapeutic resistance and induces synergistic tumor nanotherapy. *Adv Funct Mater* 2022;**32**:2107529.
77. Yuan H, Ma J, Huang W, Gong P, Shi F, Xu X, et al. Antitumor effects of a distinct sonodynamic nanosystem through enhanced induction of immunogenic cell death and ferroptosis with modulation of tumor microenvironment. *JACS Au* 2023;**3**:1507–20.
78. Zheng J, Sun Y, Long T, Yuan D, Yue S, Zhang N, et al. Sonosensitizer nanoplatform-mediated sonodynamic therapy induced immunogenic cell death and tumor immune microenvironment variation. *Drug Deliv* 2022;**29**:1164–75.
79. Zhou Y, Jiao J, Yang R, Wen B, Wu Q, Xu L, et al. Temozolomide-based sonodynamic therapy induces immunogenic cell death in glioma. *Clin Immunol* 2023;**256**:109772.
80. Tang T, Huang X, Zhang G, Liang T. Oncolytic immunotherapy: multiple mechanisms of oncolytic peptides to confer anticancer immunity. *J Immunother Cancer* 2022;**10**:e005065.
81. Yamazaki T, Pitt JM, Vétizou M, Marabelle A, Flores C, Rekdal Ø, et al. The oncolytic peptide LTX-315 overcomes resistance of cancers to immunotherapy with CTLA4 checkpoint blockade. *Cell Death Differ* 2016;**23**:1004–15.
82. Phung CD, Nguyen BL, Jeong JH, Chang JH, Jin SG, Choi HG, et al. Shaping the "hot" immunogenic tumor microenvironment by nanoparticles co-delivering oncolytic peptide and TGF- β 1 siRNA for boosting checkpoint blockade therapy. *Bioeng transl med* 2023;**8**:e10392.
83. Ma J, Ramachandran M, Jin C, Quijano-Rubio C, Martikainen M, Yu D, et al. Characterization of virus-mediated immunogenic cancer cell death and the consequences for oncolytic virus-based immunotherapy of cancer. *Cell Death Dis* 2020;**11**:48.
84. Garofalo M, Villa A, Rizzi N, Kuryk L, Rinner B, Cerullo V, et al. Extracellular vesicles enhance the targeted delivery of immunogenic oncolytic adenovirus and paclitaxel in immunocompetent mice. *J Control Release* 2019;**294**:165–75.
85. Li J, Zhou S, Yu J, Cai W, Yang Y, Kuang X, et al. Low dose shikonin and anthracyclines coloaded liposomes induce robust immunogenetic cell death for synergistic chemo-immunotherapy. *J Control Release* 2021;**335**:306–19.
86. Liu Q, Chen F, Hou L, Shen L, Zhang X, Wang D, et al. Nanocarrier-mediated chemo-immunotherapy arrested cancer progression and induced tumor dormancy in desmoplastic melanoma. *ACS Nano* 2018;**12**:7812–25.
87. He C, Duan X, Guo N, Chan C, Poon C, Weichselbaum RR, et al. Core-shell nanoscale coordination polymers combine chemotherapy and photodynamic therapy to potentiate checkpoint blockade cancer immunotherapy. *Nat Commun* 2016;**7**:12499.
88. Huang Y, Wei D, Wang B, Tang D, Cheng A, Xiao S, et al. NIR-II light evokes DNA cross-linking for chemotherapy and immunogenic cell death. *Acta Biomater* 2023;**160**:198–210.
89. Chen Q, Liu L, Lu Y, Chen X, Zhang Y, Zhou W, et al. Tumor microenvironment-triggered aggregated magnetic nanoparticles for reinforced image-guided immunogenic chemotherapy. *Adv Sci* 2019;**6**:1802134.
90. Yan S, Zeng X, Tang Y, Liu BF, Wang Y, Liu X. Activating antitumor immunity and antimetastatic effect through polydopamine-encapsulated core-shell upconversion nanoparticles. *Adv Mater* 2019;**31**:e1905825.
91. Beik J, Abed Z, Ghoreishi FS, Hosseini-Nami S, Mehrzadi S, Shakeri-Zadeh A, et al. Nanotechnology in hyperthermia cancer therapy: from fundamental principles to advanced applications. *J Control Release* 2016;**235**:205–21.
92. Wang Z, Zhang F, Shao D, Chang Z, Wang L, Hu H, et al. Janus nanobullets combine photodynamic therapy and magnetic hyperthermia to potentiate synergetic anti-metastatic immunotherapy. *Adv Sci* 2019;**6**:1901690.
93. Chitphet K, Geary SM, Chan CHF, Simons AL, Weiner GJ, Salem AK. Combining doxorubicin-loaded pegylated poly(lactide-co-glycolide) nanoparticles with checkpoint inhibition safely enhances therapeutic efficacy in a melanoma model. *ACS Biomater Sci Eng* 2020;**6**:2659–67.
94. Yu W, He X, Yang Z, Yang X, Xiao W, Liu R, et al. Sequentially responsive biomimetic nanoparticles with optimal size in combination with checkpoint blockade for cascade synergetic treatment of breast cancer and lung metastasis. *Biomaterials* 2019;**217**:119309.
95. Tang X, Rao J, Yin S, Wei J, Xia C, Li M, et al. PD-L1 knockdown via hybrid micelle promotes paclitaxel induced cancer-immunity cycle for melanoma treatment. *Eur J Pharmaceut Sci* 2019;**127**:161–74.
96. Phung CD, Nguyen HT, Choi JY, Pham TT, Acharya S, Timilshina M, et al. Reprogramming the T cell response to cancer by simultaneous, nanoparticle-mediated PD-L1 inhibition and immunogenic cell death. *J Control Release* 2019;**315**:126–38.
97. Tu K, Deng H, Kong L, Wang Y, Yang T, Hu Q, et al. Reshaping tumor immune microenvironment through acidity-responsive nanoparticles featured with CRISPR/Cas9-mediated programmed death-ligand 1 attenuation and chemotherapeutics-induced immunogenic cell death. *ACS Appl Mater Interfaces* 2020;**12**:16018–30.
98. Moon Y, Shim MK, Choi J, Yang S, Kim J, Yun WS, et al. Anti-PD-L1 peptide-conjugated prodrug nanoparticles for targeted cancer immunotherapy combining PD-L1 blockade with immunogenic cell death. *Theranostics* 2022;**12**:1999–2014.
99. De Silva P, Aiello M, Gu-Trantien C, Migliori E, Willard-Gallo K, CJJoc Solinas. Targeting CTLA-4 in cancer: is it the ideal companion for PD-1 blockade immunotherapy combinations?. *Int J Cancer* 2021;**149**:31–41.
100. Rios-Doria J, Durham N, Wetzel L, Rothstein R, Chesebrough J, Holowekyj N, et al. Doxil synergizes with cancer immunotherapies to enhance antitumor responses in syngeneic mouse models. *Neoplasia* 2015;**17**:661–70.
101. Müller D. Targeting co-stimulatory receptors of the TNF superfamily for cancer immunotherapy. *BioDrugs* 2023;**37**:21–33.
102. Dong X, Yang A, Bai Y, Kong D, Lv F. Dual fluorescence imaging-guided programmed delivery of doxorubicin and CpG nanoparticles to modulate tumor microenvironment for effective chemo-immunotherapy. *Biomaterials* 2020;**230**:119659.
103. Li J, Zhao M, Liang W, Wu S, Wang Z, Wang D. Codelivery of Shikonin and siTGF- β for enhanced triple negative breast cancer chemo-immunotherapy. *J Control Release* 2022;**342**:308–20.
104. Wang-Bishop L, Wehbe M, Shae D, James J, Hacker BC, Garland K, et al. Potent STING activation stimulates immunogenic cell death to enhance antitumor immunity in neuroblastoma. *J Immunother Cancer* 2020;**8**.
105. Mei L, Liu Y, Rao J, Tang X, Li M, Zhang Z, et al. Enhanced tumor retention effect by click chemistry for improved cancer immunotherapy. *ACS Appl Mater Interfaces* 2018;**10**:17582–93.
106. Kim D, Byun J, Park J, Lee Y, Shim G, Oh YK. Biomimetic polymeric nanoparticle-based photodynamic immunotherapy and

- protection against tumor rechallenge. *Biomater Sci* 2020;**8**:1106–16.
107. Wang Y, Wang Z, Chen B, Yin Q, Pan M, Xia H, et al. Cooperative self-assembled nanoparticle induces sequential immunogenic cell death and toll-like receptor activation for synergistic chemo-immunotherapy. *Nano Lett* 2021;**21**:4371–80.
 108. Labadie BW, Bao R, Luke JJCCR. Reimagining IDO pathway inhibition in cancer immunotherapy via downstream focus on the tryptophan–kynurenine–aryl hydrocarbon axis. *Clin Cancer Res* 2019;**25**:1462–71.
 109. Le Naour J, Galluzzi L, Zitvogel L, Kroemer G, Vacchelli E. Trial watch: IDO inhibitors in cancer therapy. *OncImmunology* 2020;**9**:1777625.
 110. Lu J, Liu X, Liao YP, Salazar F, Sun B, Jiang W, et al. Nano-enabled pancreas cancer immunotherapy using immunogenic cell death and reversing immunosuppression. *Nat Commun* 2017;**8**:1–14.
 111. Huang H, Jiang CT, Shen S, Liu A, Gan YJ, Tong QS, et al. Nanoenabled reversal of IDO1-mediated immunosuppression synergizes with immunogenic chemotherapy for improved cancer therapy. *Nano Lett* 2019;**19**:5356–65.
 112. Zhang D, Zhang J, Li Q, Song A, Li Z, Luan Y. Cold to hot: rational design of a minimalist multifunctional photo-immunotherapy nanoplatform toward boosting immunotherapy capability. *ACS Appl Mater Interfaces* 2019;**11**:32633–46.
 113. Shi M, Zhang J, Wang Y, Han Y, Zhao X, Hu H, et al. Blockage of the IDO1 pathway by charge-switchable nanoparticles amplifies immunogenic cell death for enhanced cancer immunotherapy. *Acta Biomater* 2022;**150**:353–66.
 114. Chattopadhyay S, Liu YH, Fang ZS, Lin CL, Lin JC, Yao BY, et al. Synthetic immunogenic cell death mediated by intracellular delivery of STING agonist nanoshells enhances anticancer chemo-immunotherapy. *Nano Lett* 2020;**20**:2246–56.
 115. Bausart M, Rodella G, Dumont M, Ucakar B, Vanvarenberg K, Malfanti A, et al. Combination of local immunogenic cell death-inducing chemotherapy and DNA vaccine increases the survival of glioblastoma-bearing mice. *Nanomedicine* 2023;**50**:102681.
 116. Bagher M, Larsson-Callerfelt AK, Rosmark O, Hallgren O, Bjermer L, Westergren-Thorsson GJCC, et al. Mast cells and mast cell tryptase enhance migration of human lung fibroblasts through protease-activated receptor 2. *Cell Commun Signal* 2018;**16**:1–13.
 117. He Y, Wu S, Yuan Y, Sun Y, Ai Q, Zhou R, et al. Remodeling tumor immunosuppression with molecularly imprinted nanoparticles to enhance immunogenic cell death for cancer immunotherapy. *J Control Release* 2023;**362**:44–57.
 118. Zhou F, Feng B, Yu H, Wang D, Wang T, Ma Y, et al. Tumor microenvironment-activatable prodrug vesicles for nanoenabled cancer chemioimmunotherapy combining immunogenic cell death induction and CD47 blockade. *Adv Mater* 2019;**31**:e1805888.
 119. Lee EJ, Nam GH, Lee NK, Kih M, Koh E, Kim YK, et al. Nanocage-therapeutics prevailing phagocytosis and immunogenic cell death awakens immunity against cancer. *Adv Mater* 2018;**30**.
 120. Zhao M, Li J, Chen F, Han Y, Chen D, Hu H. Engineering nanoparticles boost TNBC therapy by CD24 blockade and mitochondrial dynamics regulation. *J Control Release* 2023;**355**:211–27.
 121. Barkal AA, Brewer RE, Markovic M, Kowarsky M, Barkal SA, Zaro BW, et al. CD24 signalling through macrophage Siglec-10 is a target for cancer immunotherapy. *Nature* 2019;**572**:392–6.
 122. Wei B, Pan J, Yuan R, Shao B, Wang Y, Guo X, et al. Polarization of tumor-associated macrophages by nanoparticle-loaded *Escherichia coli* combined with immunogenic cell death for cancer Immunotherapy. *Nano Lett* 2021;**21**:4231–40.
 123. Gao Z, Li Y, Wang F, Huang T, Fan K, Zhang Y, et al. Mitochondrial dynamics controls anti-tumour innate immunity by regulating CHIP–IRF1 axis stability. *Nat Commun* 2017;**8**:1805.
 124. Zhao M, Li J, Liu J, Xu M, Ji H, Wu S, et al. Charge-switchable nanoparticles enhance cancer immunotherapy based on mitochondrial dynamic regulation and immunogenic cell death induction. *J Control Release* 2021;**335**:320–32.
 125. Wang R, Hua Y, Wu H, Wang J, Xiao YC, Chen X, et al. Hydroxyapatite nanoparticles promote TLR4 agonist-mediated anti-tumor immunity through synergically enhanced macrophage polarization. *Acta Biomater* 2023;**164**:626–40.
 126. Semenza GL. Hypoxia-inducible factors in physiology and medicine. *Cell* 2012;**148**:399–408.
 127. Qian C, Yu J, Chen Y, Hu Q, Xiao X, Sun W, et al. Light-activated hypoxia-responsive nanocarriers for enhanced anticancer therapy. *Adv Mater* 2016;**28**:3313–20.
 128. Feng L, Cheng L, Dong Z, Tao D, Barnhart TE, Cai W, et al. Theranostic liposomes with hypoxia-activated prodrug to effectively destruct hypoxic tumors post-photodynamic therapy. *ACS Nano* 2017;**11**:927–37.
 129. Mai X, Zhang Y, Fan H, Song W, Chang Y, Chen B, et al. Integration of immunogenic activation and immunosuppressive reversion using mitochondrial-respiration-inhibited platelet-mimicking nanoparticles. *Biomaterials* 2020;**232**:119699.
 130. Li W, Yang J, Luo L, Jiang M, Qin B, Yin H, et al. Targeting photodynamic and photothermal therapy to the endoplasmic reticulum enhances immunogenic cancer cell death. *Nat Commun* 2019;**10**:3349.
 131. Amini MA, Abbasi AZ, Cai P, Lip H, Gordijo CR, Li J, et al. Combining tumor microenvironment modulating nanoparticles with doxorubicin to enhance chemotherapeutic efficacy and boost anti-tumor immunity. *J Natl Cancer Inst* 2019;**111**:399–408.
 132. Wang Y, Wang Q, Wang X, Yao P, Dai Q, Qi X, et al. Docetaxel-loaded pH/ROS dual-responsive nanoparticles with self-supplied ROS for inhibiting metastasis and enhancing immunotherapy of breast cancer. *J Nanobiotechnol* 2023;**21**:286.
 133. He H, Liu L, Liang R, Zhou H, Pan H, Zhang S, et al. Tumor-targeted nanoplatform for *in situ* oxygenation-boosted immunogenic phototherapy of colorectal cancer. *Acta Biomater* 2020;**104**:188–97.
 134. Zetrini AE, Lip H, Abbasi AZ, Alradwan I, Ahmed T, He C, et al. Remodeling tumor immune microenvironment by using polymer-lipid-manganese dioxide nanoparticles with radiation therapy to boost immune response of castration-resistant prostate cancer. *Research* 2023;**6**:247. Washington, DC.
 135. Yu Z, Guo J, Hu M, Gao Y, Huang L. Icaritin exacerbates mitophagy and synergizes with doxorubicin to induce immunogenic cell death in hepatocellular carcinoma. *ACS Nano* 2020;**14**:4816–28.
 136. Li J, Cai W, Yu J, Zhou S, Li X, He Z, et al. Autophagy inhibition recovers deficient ICD-based cancer immunotherapy. *Biomaterials* 2022;**287**:121651.
 137. Liu Q, Zhu H, Tiruthani K, Shen L, Chen F, Gao K, et al. Nanoparticle-mediated trapping of wnt family member 5a in tumor microenvironments enhances immunotherapy for B-Raf proto-oncogene mutant melanoma. *ACS Nano* 2018;**12**:1250–61.
 138. Hong Y, Manoharan I, Suryawanshi A, Shanmugam A, Swafford D, Ahmad S, et al. Deletion of LRP5 and LRP6 in dendritic cells enhances antitumor immunity. *OncImmunology* 2016;**5**:e1115941.
 139. Hong Y, Manoharan I, Suryawanshi A, Majumdar T, Angus-Hill ML, Koni PA, et al. β -Catenin promotes regulatory T-cell responses in tumors by inducing vitamin A metabolism in dendritic cells. *Cancer Res* 2015;**75**:656–65.
 140. Antony F, Kang X, Pundkar C, Wang C, Mishra A, Chen P, et al. Targeting β -catenin using XAV939 nanoparticle promotes immunogenic cell death and suppresses conjunctival melanoma progression. *Int J Pharm* 2023;**640**:123043.
 141. Kopecka J, Porto S, Lusa S, Gazzano E, Salzano G, Pinzón-Daza ML, et al. Zoledronic acid-encapsulating self-assembling nanoparticles and doxorubicin: a combinatorial approach to overcome simultaneously chemoresistance and immunoresistance in breast tumors. *Oncotarget* 2016;**7**:20753–72.
 142. Vacchelli E, Ma Y, Baracco EE, Sistigu A, Enot DP, Pietrocola F, et al. Chemotherapy-induced antitumor immunity requires formyl peptide receptor 1. *Science* 2015;**350**:972–8.
 143. Xu C, Yu Y, Sun Y, Kong L, Yang C, Hu M, et al. Transformable nanoparticle-enabled synergistic elicitation and promotion of

- immunogenic cell death for triple-negative breast cancer immunotherapy. *Adv Funct Mater* 2019;**29**:1905213.
144. Deng C, Jia M, Wei G, Tan T, Fu Y, Gao H, et al. Inducing optimal antitumor immune response through coadministering irdg with pirarubicin loaded nanostructured lipid carriers for breast cancer therapy. *Mol Pharm* 2017;**14**:296–309.
145. Xu X, Wang R, Li D, Xiang J, Zhang W, Shi X, et al. Guanidine-modified nanoparticles as robust BTZ delivery carriers and activators of immune responses. *J Control Release* 2023;**357**:310–8.
146. Deng H, Zhou Z, Yang W, Lin LS, Wang S, Niu G, et al. Endoplasmic reticulum targeting to amplify immunogenic cell death for cancer immunotherapy. *Nano Lett* 2020;**20**:1928–33.
147. Sethuraman SN, Singh MP, Patil G, Li S, Fiering S, Hoopes PJ, et al. Novel calreticulin-nanoparticle in combination with focused ultrasound induces immunogenic cell death in melanoma to enhance antitumor immunity. *Theranostics* 2020;**10**:3397–412.
148. Chao MP, Jaiswal S, Weissman-Tsukamoto R, Alizadeh AA, Gentles AJ, Volkmer J, et al. Calreticulin is the dominant pro-phagocytic signal on multiple human cancers and is counterbalanced by CD47. *Sci Transl Med* 2010;**2**:63ra94.
149. Huang FY, Lei J, Sun Y, Yan F, Chen B, Zhang L, et al. Induction of enhanced immunogenic cell death through ultrasound-controlled release of doxorubicin by liposome-microbubble complexes. *Oncol Immunology* 2018;**7**:e1446720.
150. Li Y, Liu X, Pan W, Li N, Tang B. Photothermal therapy-induced immunogenic cell death based on natural melanin nanoparticles against breast cancer. *Chem Commun* 2020;**56**:1389–92.
151. Luk BT, Zhang L. Cell membrane-camouflaged nanoparticles for drug delivery. *J Control Release* 2015;**220**:600–7.
152. Félix-Piña P, Franco Molina MA, Zarate Triviño DG, García Coronado PL, Zapata Benavides P, Rodríguez Padilla C. Antitumoral and Immunogenic capacity of β -D-glucose-reduced silver nanoparticles in breast cancer. *Int J Mol Sci* 2023;**24**:8485.
153. Zhang F, Chen F, Yang C, Wang L, Hu H, Li X, et al. Coordination and redox dual-responsive mesoporous organosilica nanoparticles amplify immunogenic cell death for cancer chemoimmunotherapy. *Small* 2021;**17**:e2100006.
154. Kaur P, Johnson A, Northcote-Smith J, Lu C, Suntharalingam KJC. Immunogenic cell death of breast cancer stem cells induced by an endoplasmic reticulum—targeting copper (II) complex. *Chem-biochem* 2020;**21**:3618–24.
155. Passeri G, Northcote-Smith J, KJRa Suntharalingam. *Delivery of an immunogenic cell death-inducing copper complex to cancer stem cells using polymeric nanoparticles*, **12**; 2022. p. 5290–9.
156. Wang Y, Ding Y, Yao D, Dong H, Ji C, Wu J, et al. Copper-based nanoscale coordination polymers augmented tumor radio-immunotherapy for immunogenic cell death induction and T-cell infiltration. *Small* 2021;**17**:2006231.
157. Huang Z, Zhang X, Luo Y, Wang Y, Zhou S. KCl nanoparticles as potential inducer of immunogenic cell death for cancer immunotherapy. *ACS Appl Bio Mater* 2023;**6**:2404–14.
158. Wei F, Ke L, Gao S, Karges J, Wang J, Chen Y, et al. *In situ* oxidative polymerization of platinum(IV) prodrugs in pore-confined spaces of CaCO₃ nanoparticles for cancer chemoimmunotherapy. *Chem Sci* 2023;**14**:7005–15.
159. Li J, Ding B, Tan J, Chen H, Meng Q, Li X, et al. Sodium citrate nanoparticles induce dual-path pyroptosis for enhanced antitumor immunotherapy through synergistic ion overload and metabolic disturbance. *Nano Lett* 2023;**23**:10034–43.
160. Zhuang W-R, Wang Y, Lei Y, Zuo L, Jiang A, Wu G, et al. Phytochemical engineered bacterial outer membrane vesicles for photodynamic effects promoted immunotherapy. *Nano Lett* 2022;**22**:4491–500.
161. Kim OY, Park HT, Dinh NTH, Choi SJ, Lee J, Kim JH, et al. Bacterial outer membrane vesicles suppress tumor by interferon- γ -mediated antitumor response. *Nat Commun* 2017;**8**:626.
162. Liu XZ, Wen ZJ, Li YM, Sun WR, Hu XQ, Zhu JZ, et al. Bio-engineered bacterial membrane vesicles with multifunctional nanoparticles as a versatile platform for cancer immunotherapy. *ACS Appl Mater Interfaces* 2023;**15**:3744–59.
163. Song W, Anselmo AC, Huang L. Nanotechnology intervention of the microbiome for cancer therapy. *Nat Nanotechnol* 2019;**14**:1093–103.
164. He T, Wang L, Gou S, Lu L, Liu G, Wang K, et al. Enhanced immunogenic cell death and antigen presentation via engineered bifidobacterium bifidum to boost chemo-immunotherapy. *ACS Nano* 2023;**17**:9953–71.
165. Dai Z, Wang Q, Tang J, Wu M, Li H, Yang Y, et al. Immune-regulating bimetallic metal-organic framework nanoparticles designed for cancer immunotherapy. *Biomaterials* 2022;**280**:121261.
166. Ni W, Zhu W, Wu W, Chen J, Ren P, Chen F. Nanoscale metal-organic framework-mediated immunogenic cell death boosting tumor immunotherapy. *Mater Des* 2022;**222**:111068.
167. Jeon J, Yoon B, Dey A, Song SH, Li Y, Joo H, et al. Self-immolative polymer-based immunogenic cell death inducer for regulation of redox homeostasis. *Biomaterials* 2023;**295**:122064.
168. Dai Z, Tang J, Gu Z, Wang Y, Yang Y, Yang Y, et al. Eliciting immunogenic cell death via a unitized nanoinducer. *Nano Lett* 2020;**20**:6246–54.
169. Zhang Y, Hou X, Du S, Xue Y, Yan J, Kang DD, et al. Close the cancer-immunity cycle by integrating lipid nanoparticle-mRNA formulations and dendritic cell therapy. *Nat Nanotechnol* 2023;**18**:1364. 1174.
170. den Brok MH, Suttmuller RP, van der Voort R, Bennis EJ, Figdor CG, Ruers TJ, et al. *In situ* tumor ablation creates an antigen source for the generation of antitumor immunity. *Cancer Res* 2004;**64**:4024–9.
171. Cao Q, Wang W, Zhou M, Huang Q, Wen X, Zhao J, et al. Induction of antitumor immunity in mice by the combination of nanoparticle-based photothermolysis and anti-PD-1 checkpoint inhibition. *Nano-medicine* 2020;**25**:102169.
172. Barker HE, Paget JT, Khan AA, Harrington KJ. The tumour micro-environment after radiotherapy: mechanisms of resistance and recurrence. *Nat Rev Cancer* 2015;**15**:409–25.
173. Sakakibara K, Sato T, Kufe DW, VonHoff DD, Kawabe T. CBP501 induces immunogenic tumor cell death and CD8 T cell infiltration into tumors in combination with platinum, and increases the efficacy of immune checkpoint inhibitors against tumors in mice. *Oncotarget* 2017;**8**:78277–88.
174. Nam GH, Lee EJ, Kim YK, Hong Y, Choi Y, Ryu MJ, et al. Combined Rho-kinase inhibition and immunogenic cell death triggers and propagates immunity against cancer. *Nat Commun* 2018;**9**:2165.
175. Sonnemann J, Gressmann S, Becker S, Wittig S, Schudde M, Beck JF. The histone deacetylase inhibitor vorinostat induces calreticulin exposure in childhood brain tumour cells *in vitro*. *Cancer Chemother Pharmacol* 2010;**66**:611–6.
176. Hossain DMS, Javaid S, Cai M, Zhang C, Sawant A, Hinton M, et al. Dinaciclib induces immunogenic cell death and enhances anti-PD1-mediated tumor suppression. *J Clin Invest* 2018;**128**:644–54.
177. Wang Q, Ju X, Wang J, Fan Y, Ren M, Zhang HJCI. Immunogenic cell death in anticancer chemotherapy and its impact on clinical studies. *Cancer Lett* 2018;**438**:17–23.
178. Vaes RD, Hendriks LE, Vooijs M, De Ruyscher DJC. Biomarkers of radiotherapy-induced immunogenic cell death. *Cells* 2021;**10**:930.
179. Yamazaki T, Vanpouille-Box C, Demaria S, Galluzzi LJTM. Immunogenic cell death driven by radiation—impact on the tumor microenvironment. *Cancer Treat Res* 2020;**180**:281–96.
180. Zhu M, Yang M, Zhang J, Yin Y, Fan X, Zhang Y, et al. Immunogenic cell death induction by ionizing radiation. *Front Immunol* 2021;**12**:705361.
181. Barker HE, Paget JTE, Khan AA, Harrington KJ. The tumour microenvironment after radiotherapy: mechanisms of resistance and recurrence. *Nat Rev Cancer* 2015;**15**:409–25.
182. Jin F, Liu D, Xu X, Ji J, Du YJJoN. Nanomaterials-based photodynamic therapy with combined treatment improves antitumor efficacy

- through boosting immunogenic cell death. *Int J Nanomed* 2021;**16**:4693–712.
183. Gomes-da-Silva LC, Kepp O, Kroemer G. Regulatory approval of photodynamic therapy: photodynamic therapy that induces immunogenic cell death. *OncImmunology* 2020;**9**:1841393.
184. Tan L, Shen X, He Z, Lu Y. The role of photodynamic therapy in triggering cell death and facilitating antitumor immunology. *Front Oncol* 2022;**12**:863107.
185. Yan B, Liu C, Wang S, Li H, Jiao J, Lee WSV, et al. Magnetic hyperthermia induces effective and genuine immunogenic tumor cell death with respect to exogenous heating. *J Mater Chem B* 2022;**10**:5364–74.
186. Jana D, Zhao Y. Strategies for enhancing cancer chemodynamic therapy performance. *Explorations* 2022;**2**:20210238.
187. Li M, Zhang W, Xu X, Liu G, Dong M, Sun K, et al. Nanosystems for chemodynamic based combination therapy: strategies and recent advances. *Front Pharmacol* 2022;**13**:1065438.
188. Yang Y, Huang J, Liu M, Qiu Y, Chen Q, Zhao T, et al. Emerging sonodynamic therapy-based nanomedicines for cancer immunotherapy. *Adv Sci* 2023;**10**:e2204365.
189. Garg AD, More S, Rufo N, Mece O, Sassano ML, Agostinis P, et al. Trial watch: immunogenic cell death induction by anticancer chemotherapeutics. *OncImmunology* 2017;**6**:e1386829.